Chapter 6. An Introduction to Spectrometric Methods

Spectroscopy: the science that deals with "*interactions of matter with electromagnetic radiation or other forms of energy*"

acoustic waves, beams of particles such as ions and electrons

(SIMS) (AES)

Spectrometry: a more restrictive term,

- ***any procedure that uses light to measure chemical concentrations.***
- **the quantitative measurement of the intensity of electromagnetic radiation at one or more wavelengths with photoelectric detector.**

What Happens When a Molecule Absorbs Light ?

Absorption of light: increases the energy of molecule

Emission of light: decreases the energy of molecule

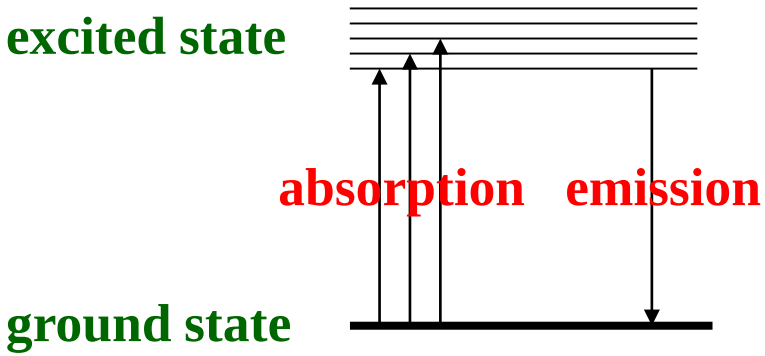

Ground state: lowest energy state of a molecule

Excitation

$$M + h\bullet \upsilon \longrightarrow M^*$$

(life time: 10^{-6} ~10^{-9} S)

Relaxation

$$M^* \longrightarrow M + \text{light (fluorescence, phosphorescence)}$$

$$\text{or} \quad M^* \longrightarrow M + \text{heat}$$

Absorption

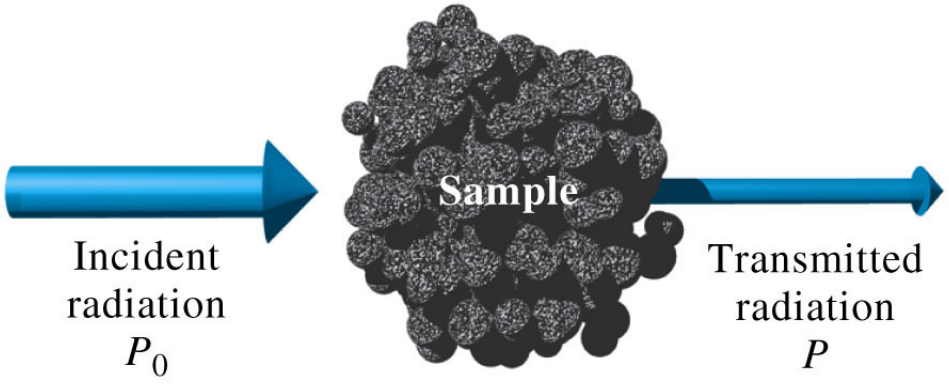

(a)

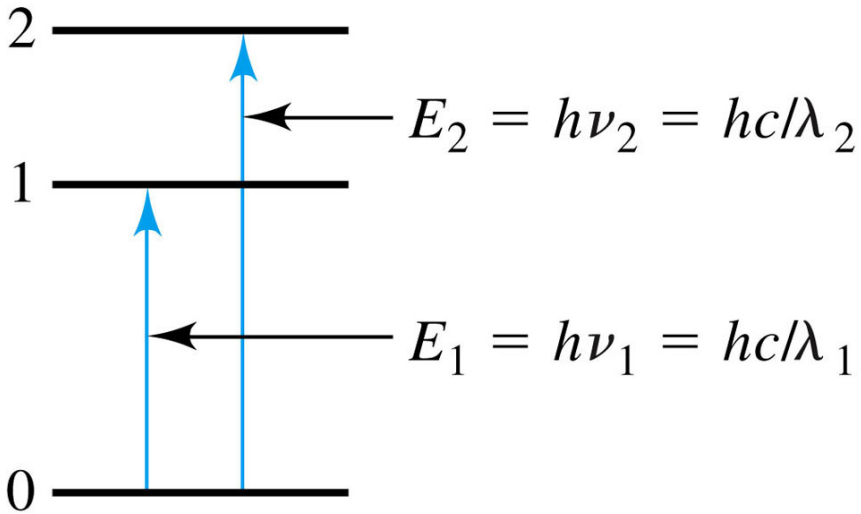

(b)

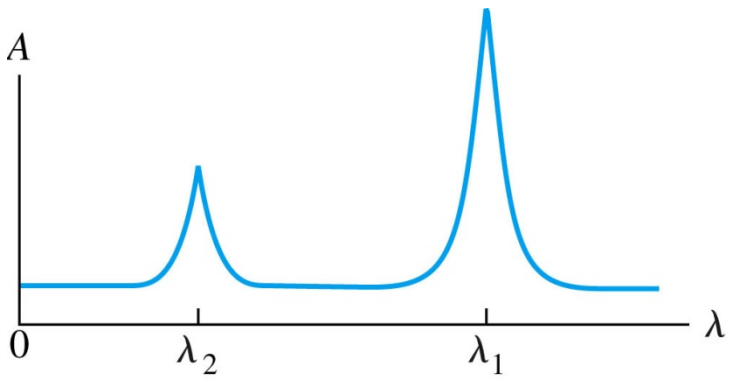

(c)

Absorption of Radiation

Absorption

(10^{-14}~10^{-15} s)

Excited state

(life-time:10^{-8} s)

Vibration

(10^{-15} s)

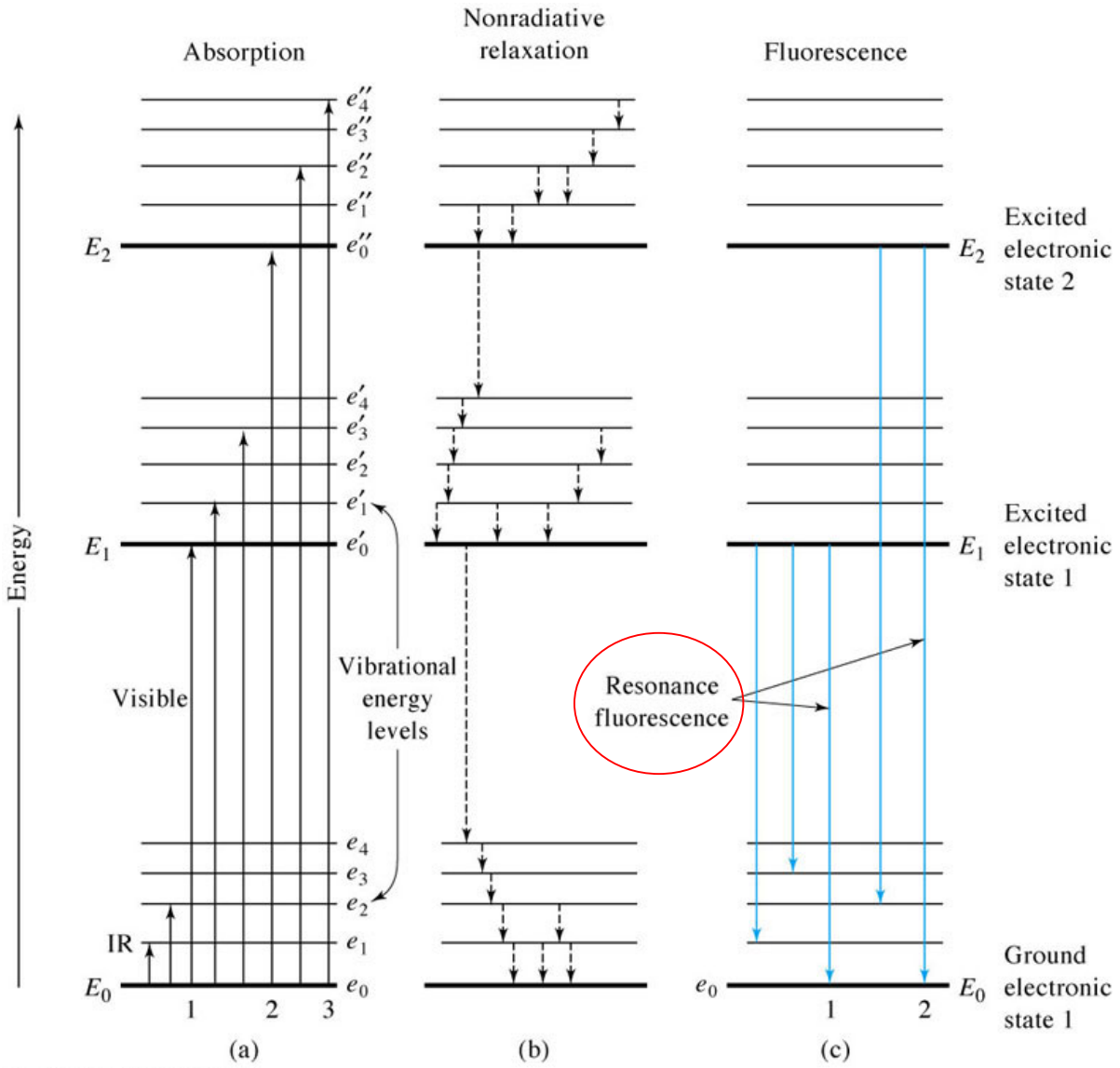

Absorption of Radiation

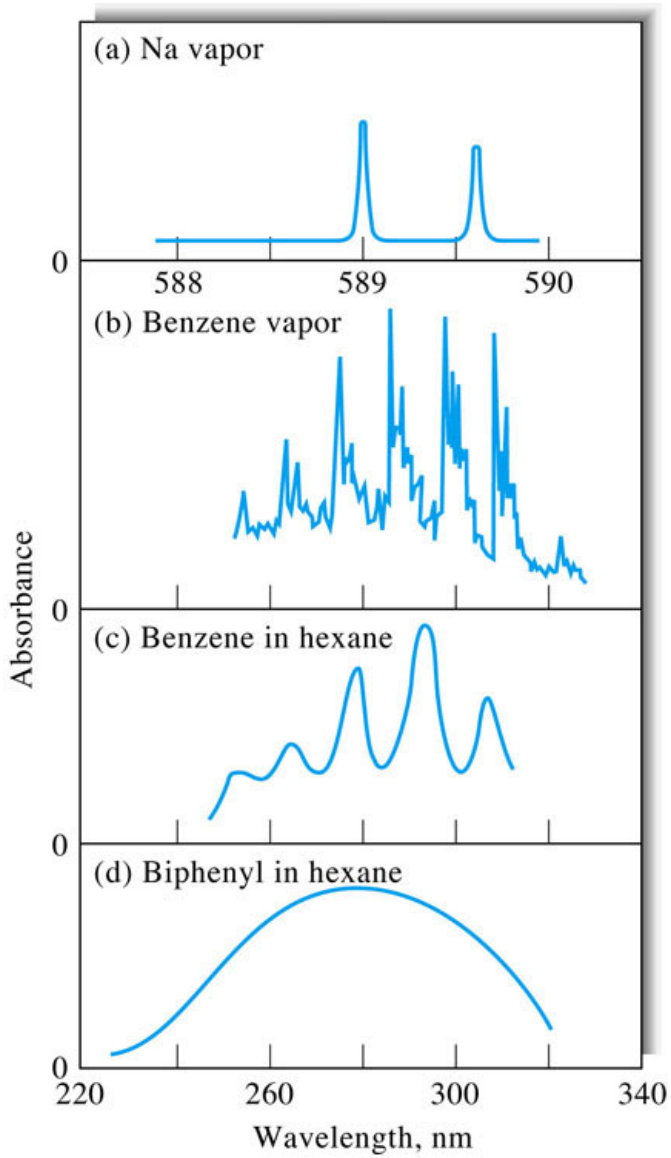

Collisional broadening

Emission or Chemiluminescence

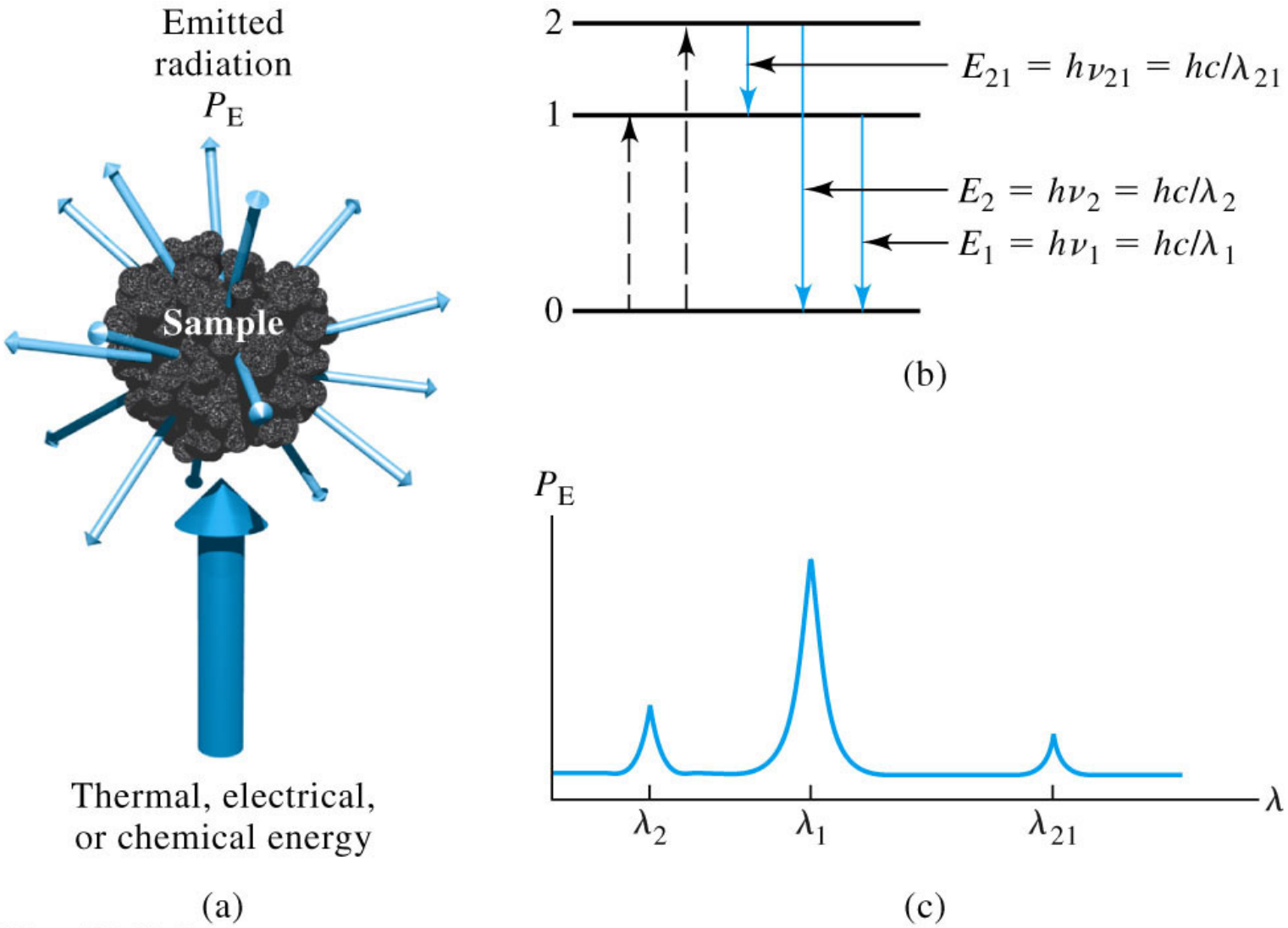

Emission of Radiation

Line spectra:

from atoms

Band spectra:

from molecules

For molecules:

$$E = E_{electronic} + E_{vibrational} + E_{rotational}$$

For atoms:

$$E = E_{electronic}$$

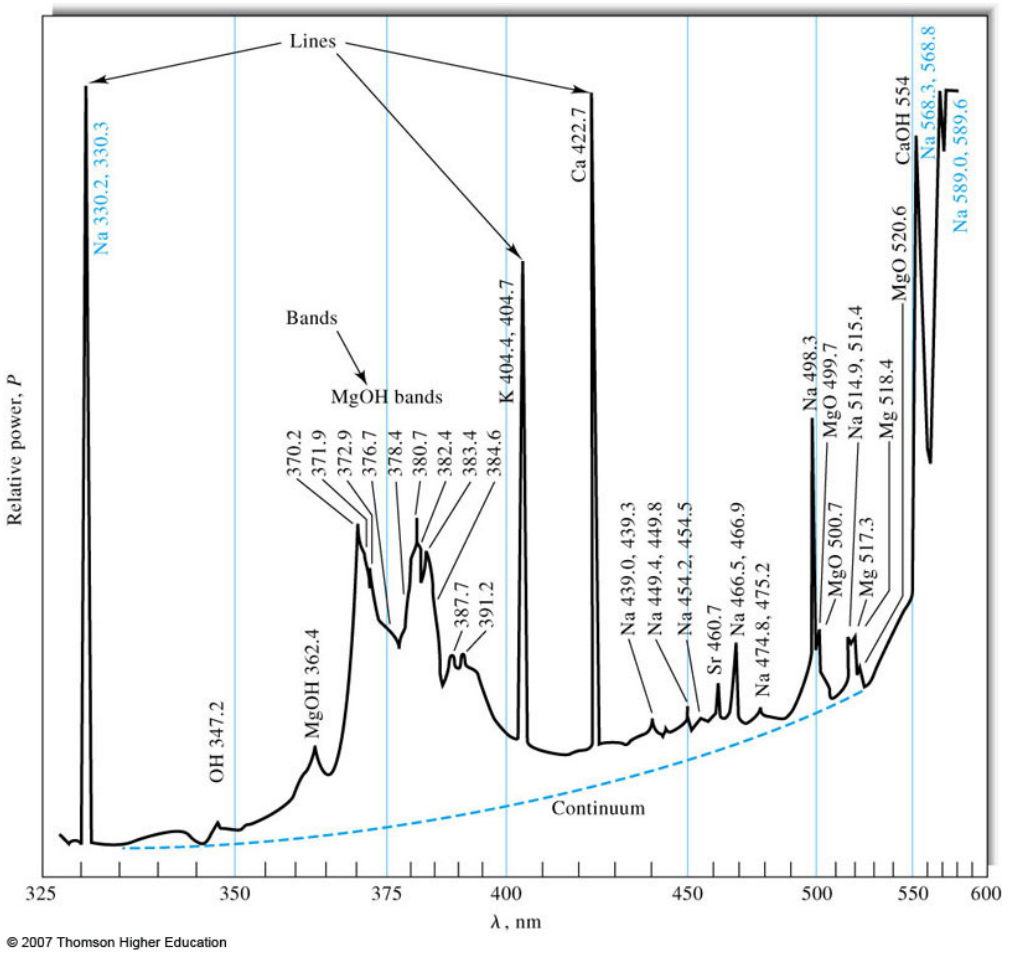

Emission of Radiation

<Sodium atom line spectra> **<Molecule band spectra>**

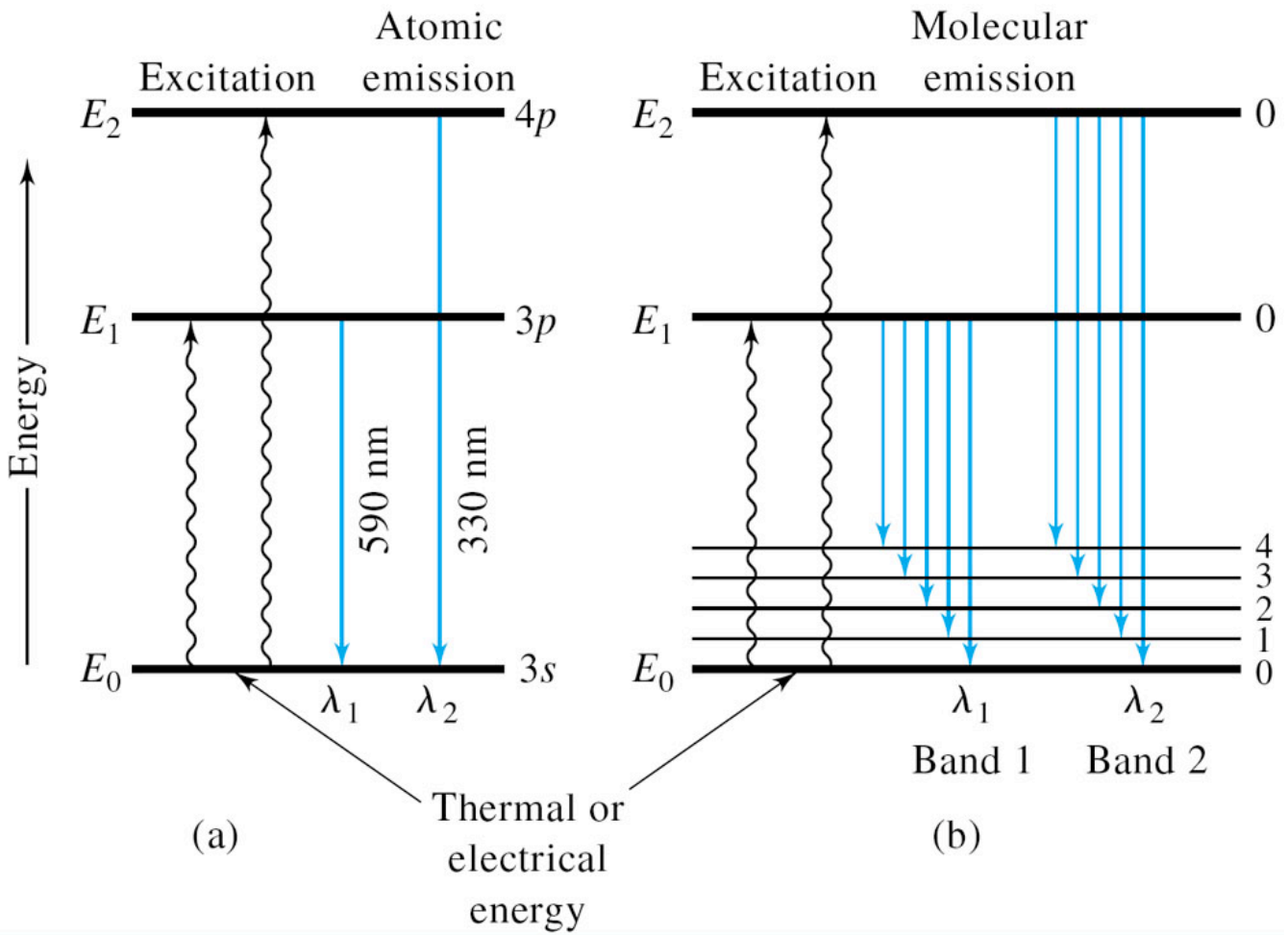

Photomluminescence

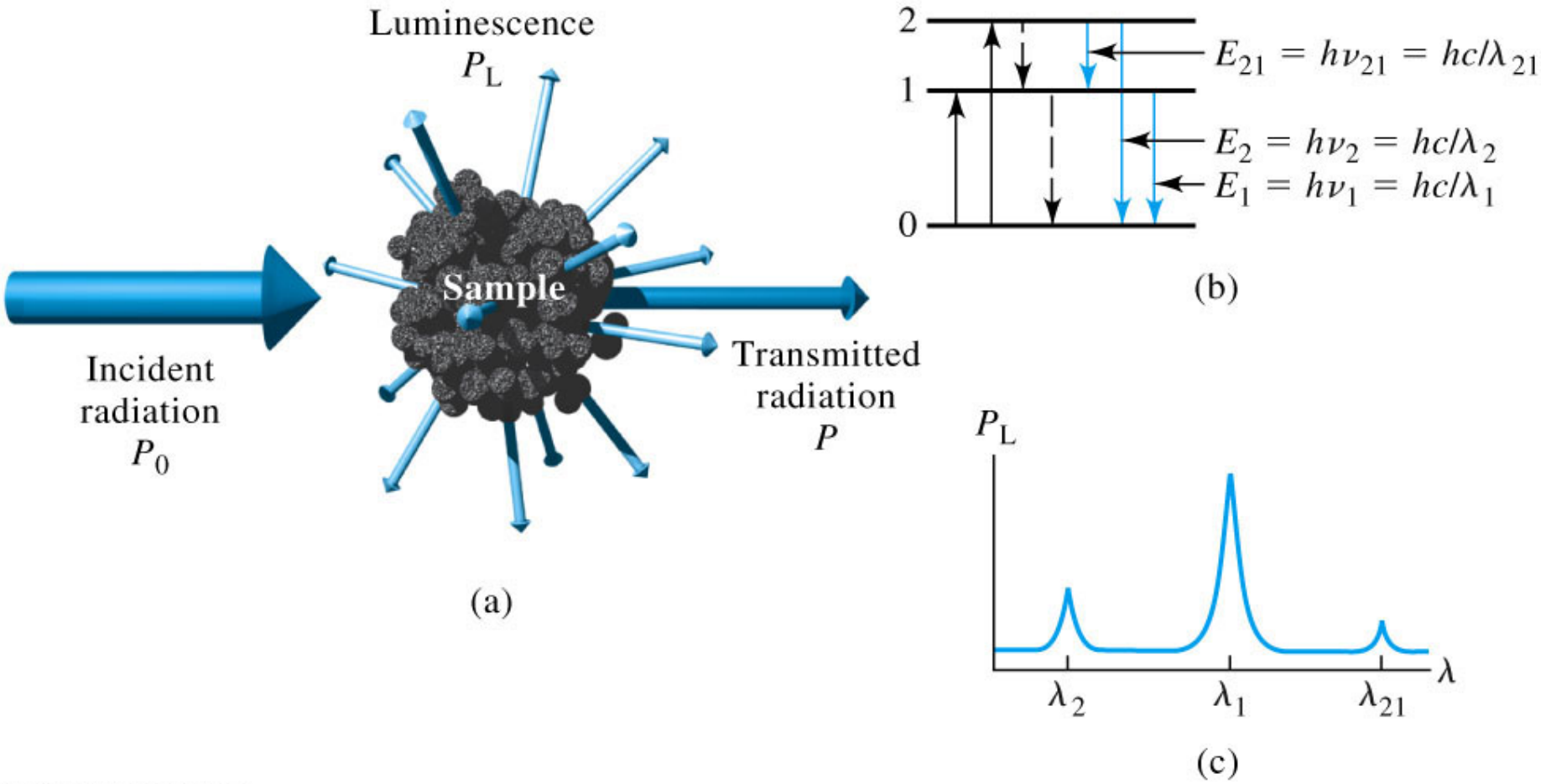

Photoluminescence

IC: raditionless transition between states with the same quantum state ($S_1 \rightarrow S_0$)

ISC: raditionless transition between states with different quantum state ($S_1 \rightarrow T_1$)

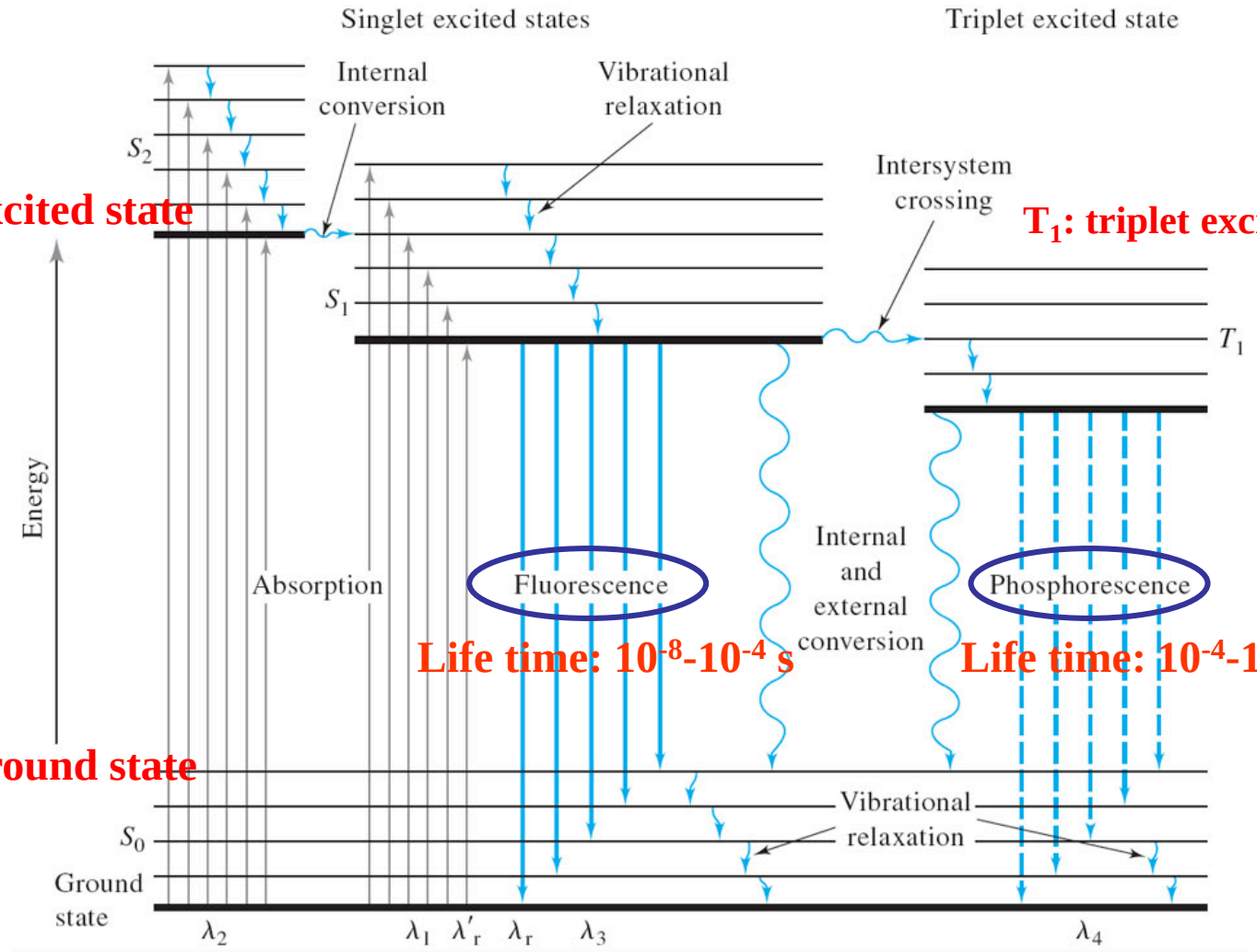

S_1: singlet excited state

T_1: triplet excited state

Life time: 10^{-8}-10^{-4} s

Life time: 10^{-4}-10^{2} s

S_0: singlet ground state

Components of Optical Spectroscopy

Absorption

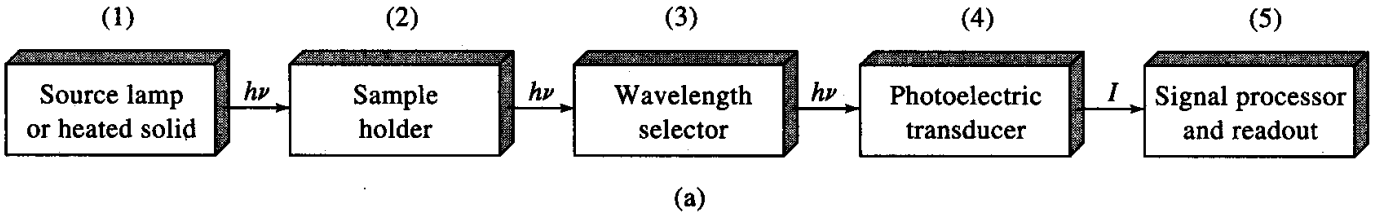

(a)

Photoluminescence

Scattering

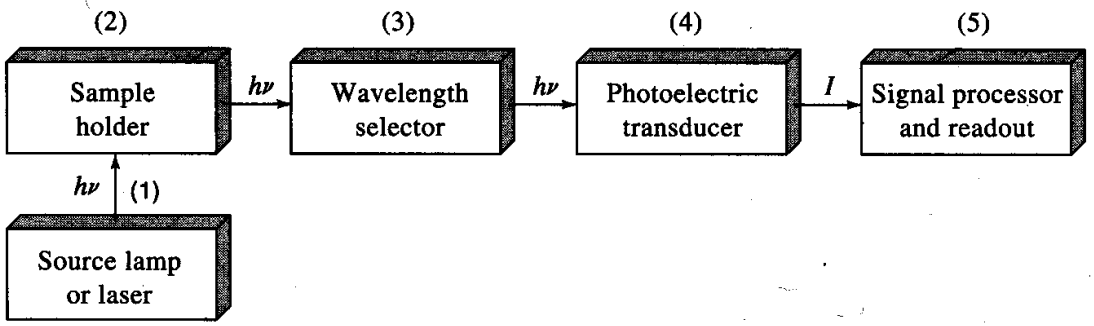

(b)

Emission

Chemiluminescence

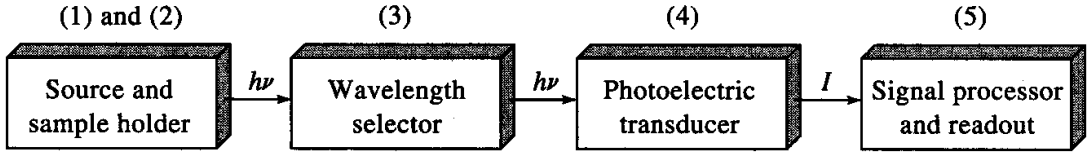

(c)

No external light source

Figure 7-1 Components of various types of instruments for optical spectroscopy: (a) absorption; (b) fluorescence, phosphorescence, and scattering; (c) emission and chemiluminescence.

Absorption of Radiation in Analytical Chemistry

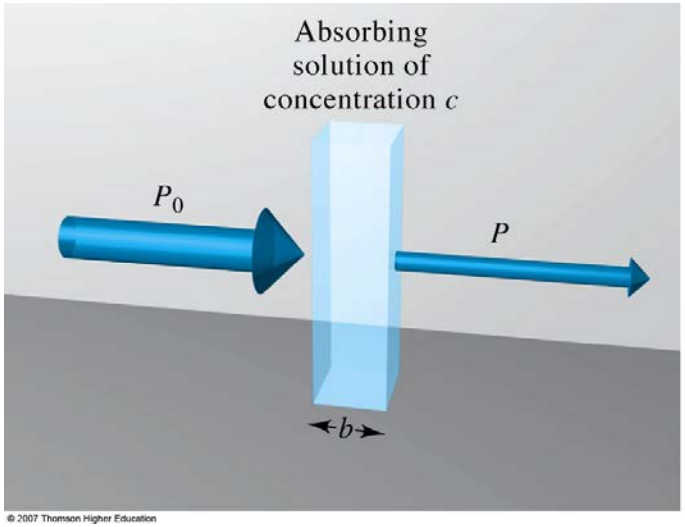

$$T = \frac{P}{P_0}$$

$$A = \log \frac{P_0}{P}$$

When light is absorbed by a sample

→the radiant power of the beam of light is decreased

Radiant power (P): **the energy per second per unit area of the light beam**

Transmittance (T): **$T = P/P_o$** **$(T = 0 \sim 1)$**

Absorbance (A), or optical density: **$A = \log (P_o/P) = -\log T$**

(if 90% light is absorbed, 10% transmitted: $T = 0.1P/P = 0.1$, $A = -\log T = 1$)

Absorption spectrum: absorbance vs wavelength

Absorption of Radiation: *Beer's Law*

The part of molecule responsible for light absorption: chromophore

Absorbance is directly proportional to the concentration

Beer-Lambert law: $A = \varepsilon bc$

ε : molar absorptivity (extinction coefficient)

characteristic of a substance that tells how much light is absorbed at a particular wavelength

b: path length

c: concentration

Beer's law works for monochromatic radiation passing through a dilute solution

Luminescence in Analytical Chemistry

Relation of emission intensity to concentration:

$$I = kP_oC$$

I: emission intensity

P_o: radiant power of incident light

C: concentration of emitting species

In FL: Higher radiation power → higher intensity → better detection

In Absorbance: Higher radiation power → no change in absorbance

(Laser-induced fluorescence; LIF) → good for the detection of trace amount

Emission intensity is not proportional to analyte concentration

at high concentration, or in the presence of significant amount of absorbing species

Self-absorption

Chapter 7. Components of Optical Instruments

Optical spectroscopic methods are based upon six phenomena

- Absorption

- Fluorescence

- Phosphorescence

- Scattering

- Emission

- Chemiluminescence

While the instruments for measuring each differ in configuration, most of their basic components are remarkably similar.

Components of Optical Spectroscopy

Sample Cell & Prism

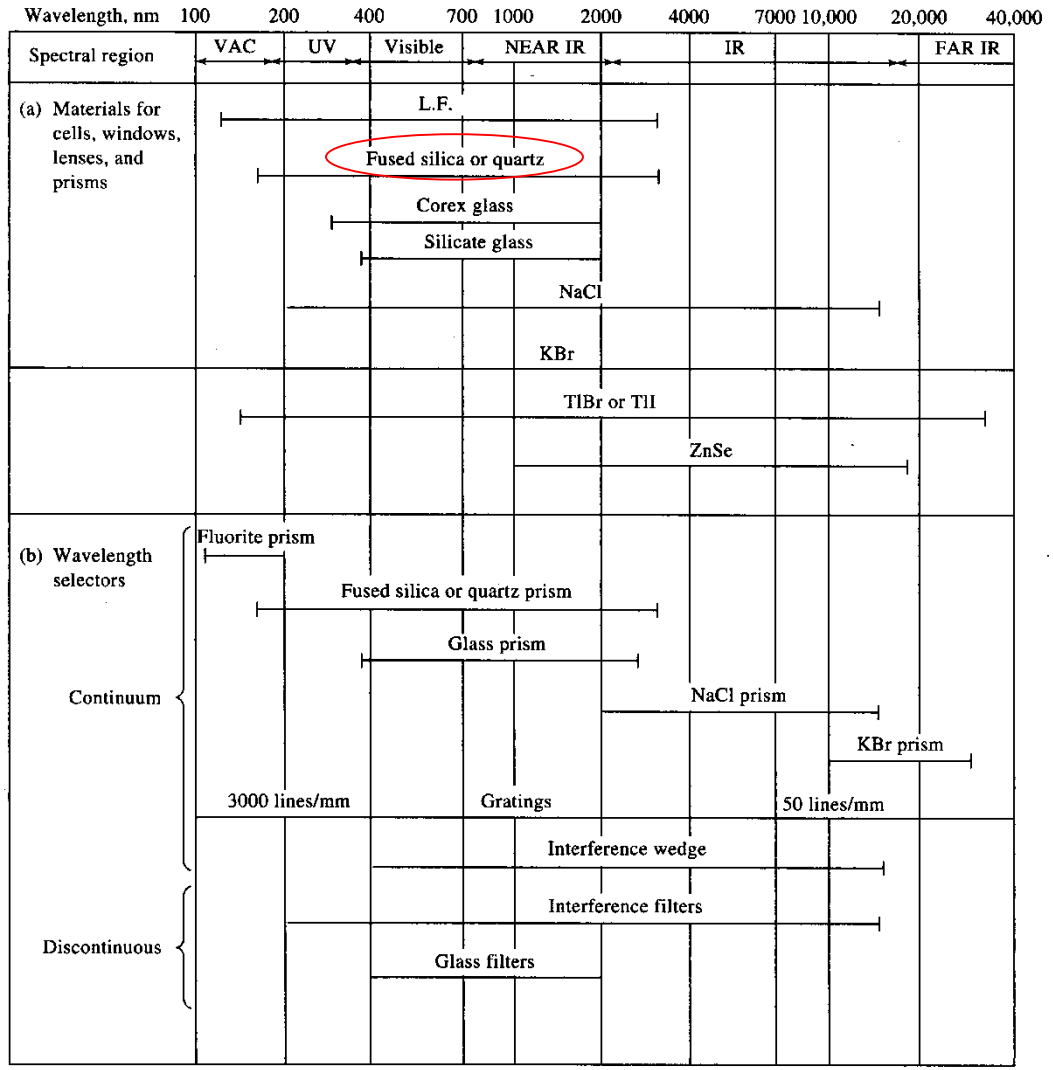

Figure 7-2 (a) Construction materials and (b) wavelength selectors for spectroscopic instruments.

Radiation Source

- should generate a beam of sufficient power (specially for FL)
- output power should be stable

Components of Optical Spectroscopy

Light Source

Light Detector

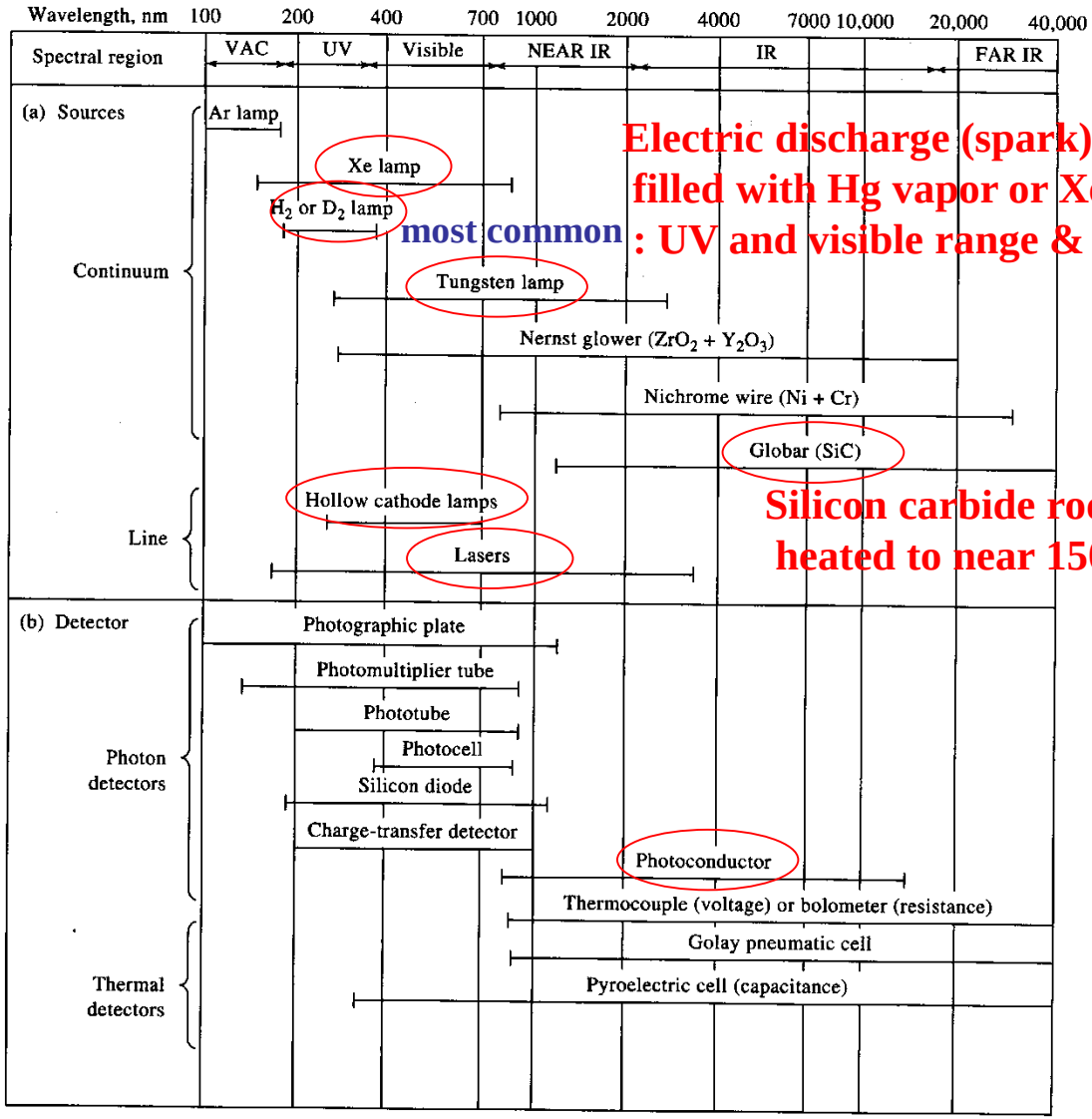

Figure 7-3 (a) Sources and (b) detectors for spectroscopic instruments.

Continuum Source

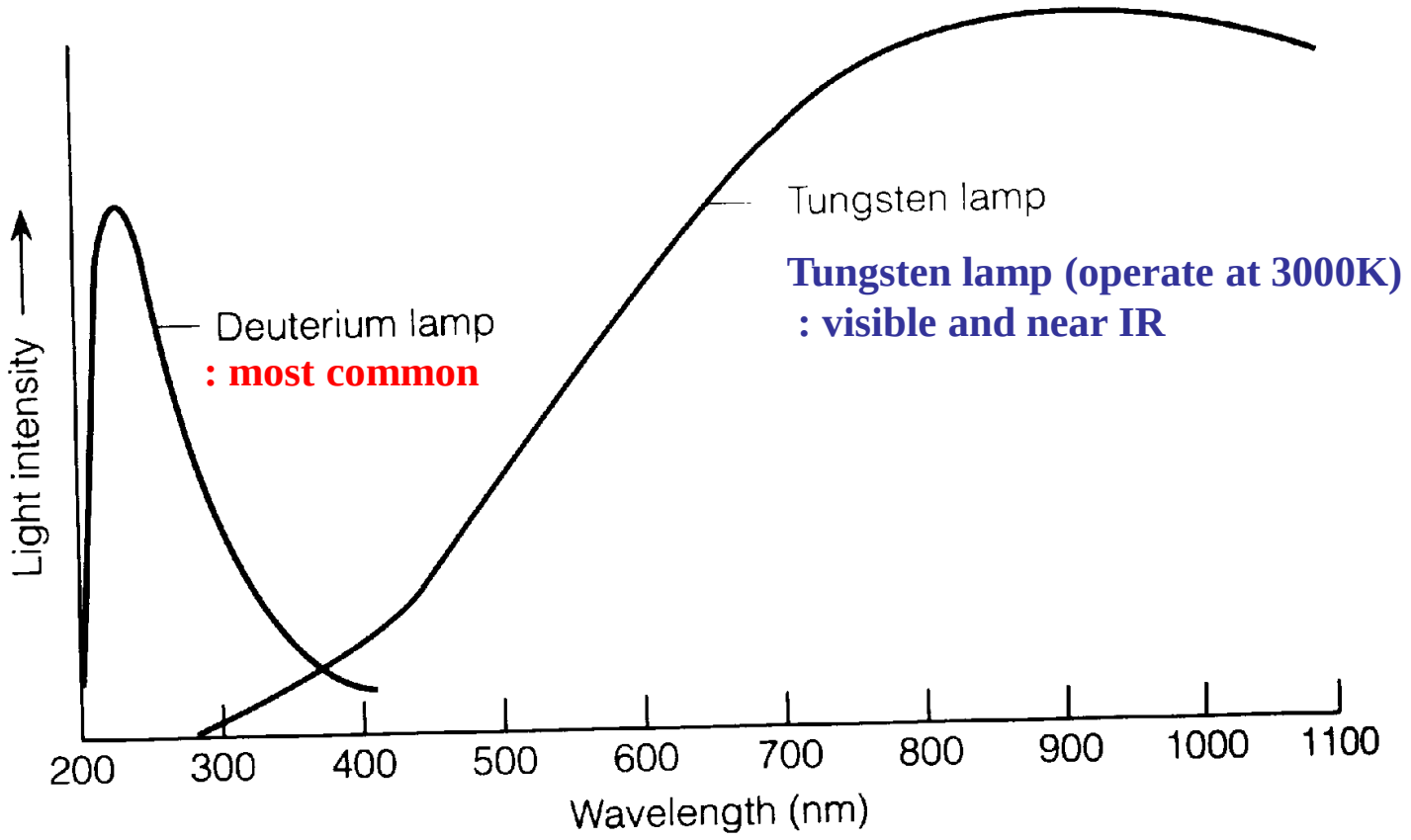

Laser

Light Amplification by Stimulated Emission of Radiation

Laser:

- **extremely intense (high intensity)**
- **highly monochromatic (narrow bandwidth of 0.01 nm or less)**
- **remarkably coherent**

The first laser: in 1960

Application of laser:

- Spectroscopy
- Detection of extremely low concentrations of species (LIF)

Laser

Laser light is obtained by three step:

- stimulated emission
- population inversion
- optical resonator or oscillator concept

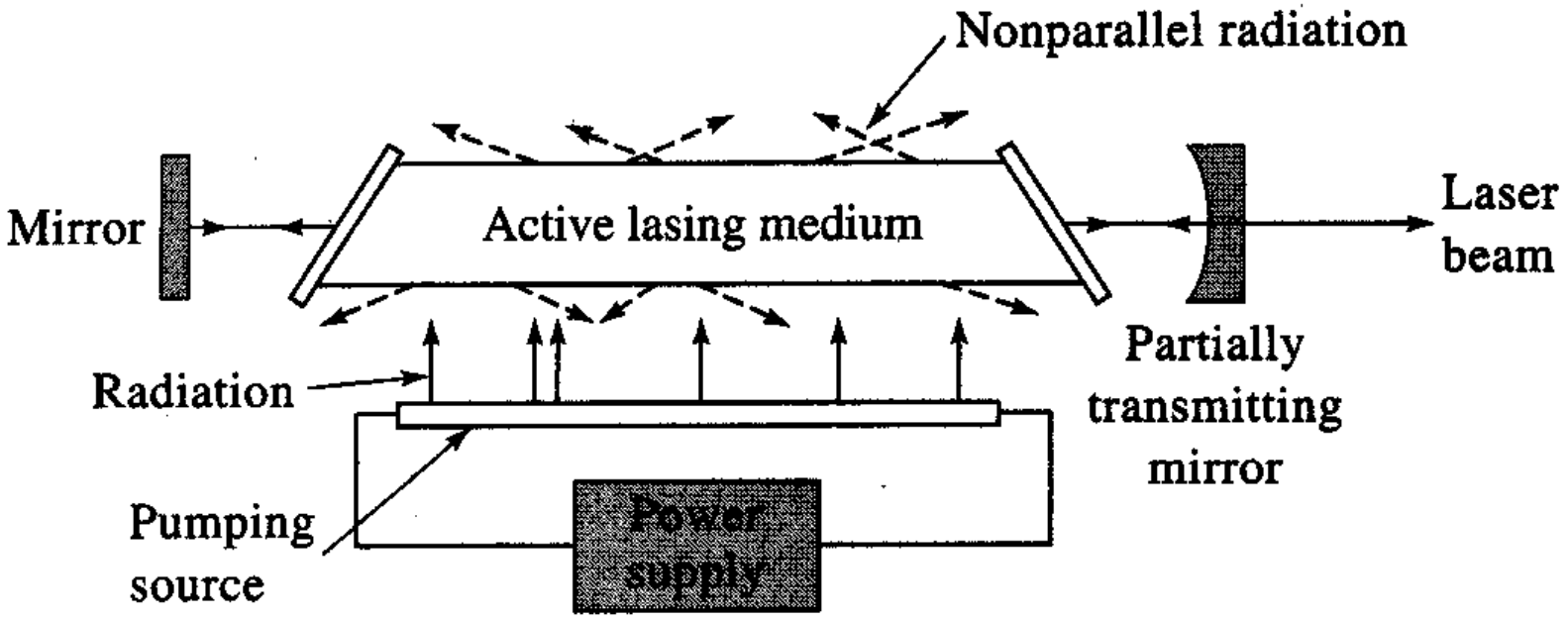

Spontaneous Emission

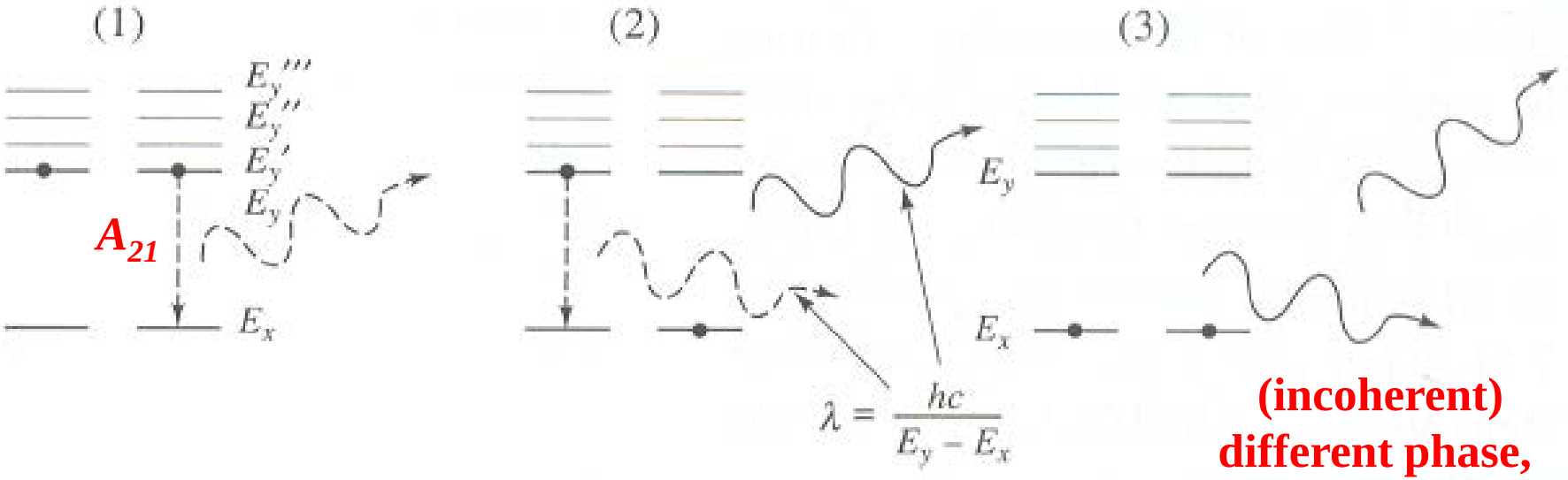

(incoherent)
different phase,
different direction

(b) Spontaneous emission **(slow)**

- A species in an excited electronic state may lose all or part of its excess energy of radiation by spontaneous emission.

- It is also important to note that *the instant at which emission occurs and the path of the resulting photon* vary from excited molecule to excited molecule because that is a random process.

- yields incoherent monochromatic radiation.

Rate of spontaneous emission = $A_{21}N_2$

(Stimulated) Absorption

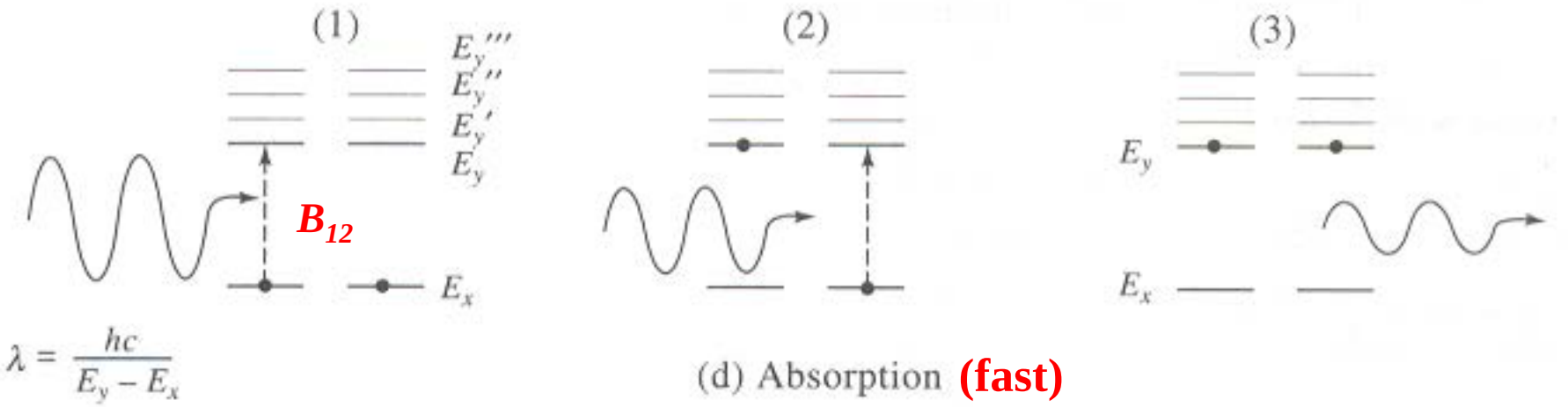

The absorption process, which compete with stimulated emission.

Absorption rate is depended on:

- **No of particles in state E_x, E_y**
- **intensity of radiation, I(v)**
- **inherent probability of the transition (B_{12})—absorption coefficient**

Rate of absorption = B_{12} I(v) N_1

Stimulated Emission

(coherent)
same phase,
same direction

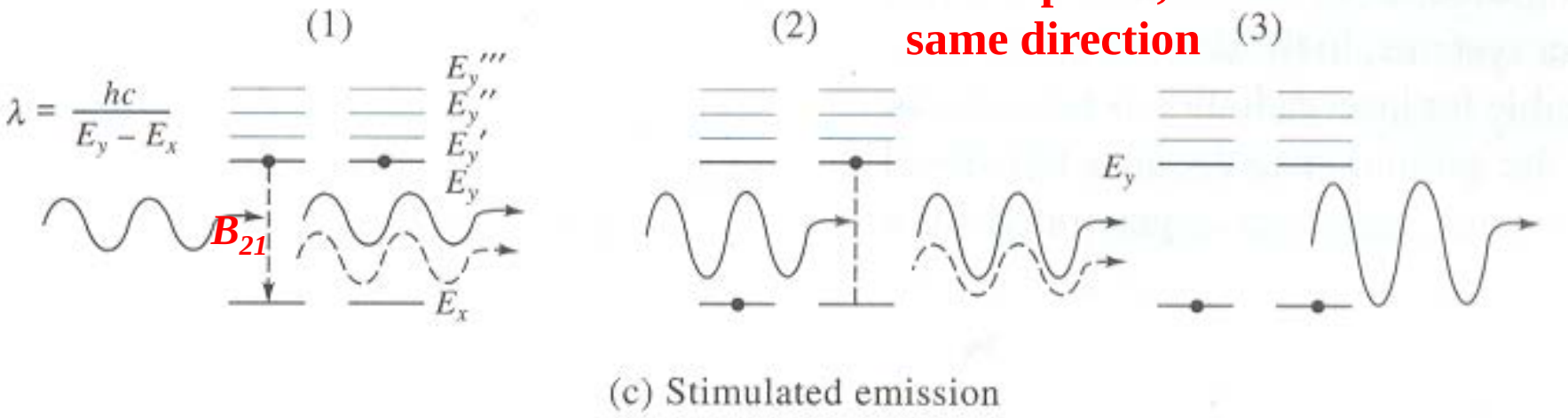

(c) Stimulated emission

- The excited laser species are struck by photons that have precisely the same energies as the photons produced by spontaneous emission
-Collision of this type cause the excited species to relax immediately to lower energy level and stimulate emission

- The emitted photon travels in exactly same direction and precisely in phase.
- The stimulated emission is totally coherent with the incoming radiation

Rate of stimulated emission = B_{21} I(ν) N_2

Population Inversion - Pumping

In order to have light amplification, it is necessary that the # of photons produced by stimulated emission exceed the # lost by absorption.

N1>N2
Non-inverted population

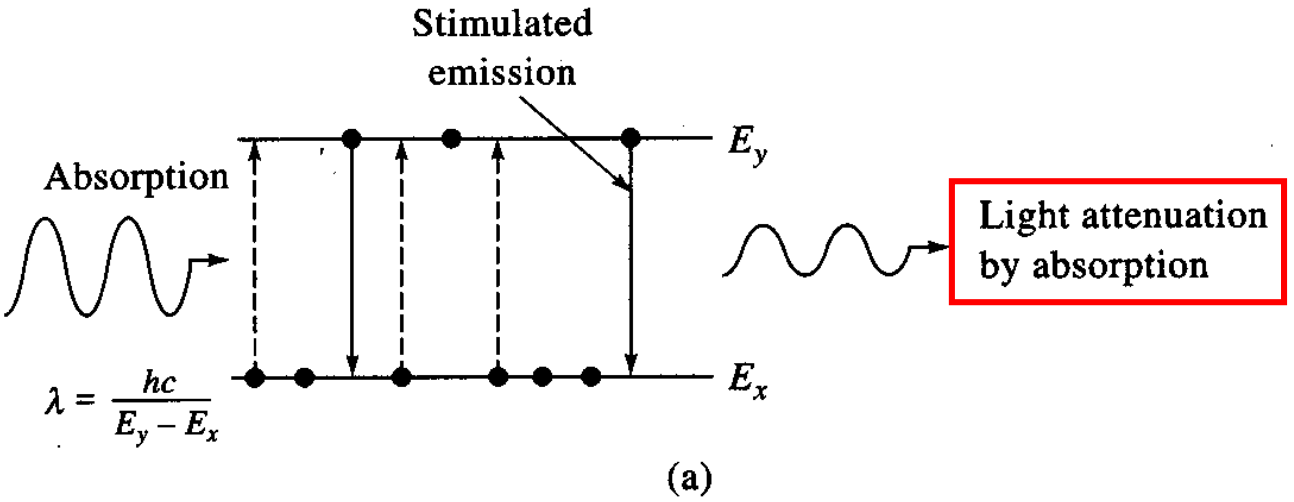

N1<N2
inverted population

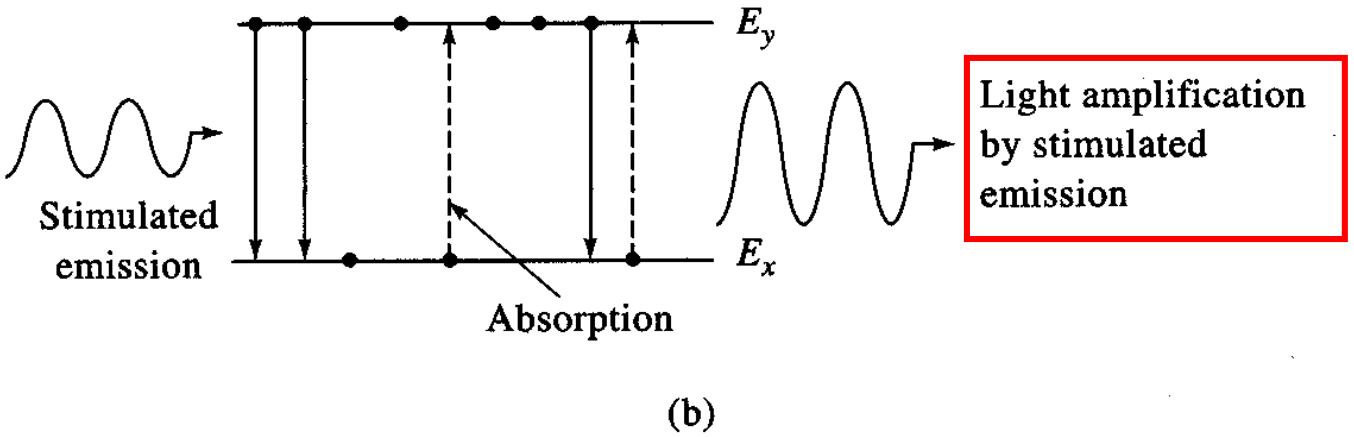

Three-Level Laser Systems

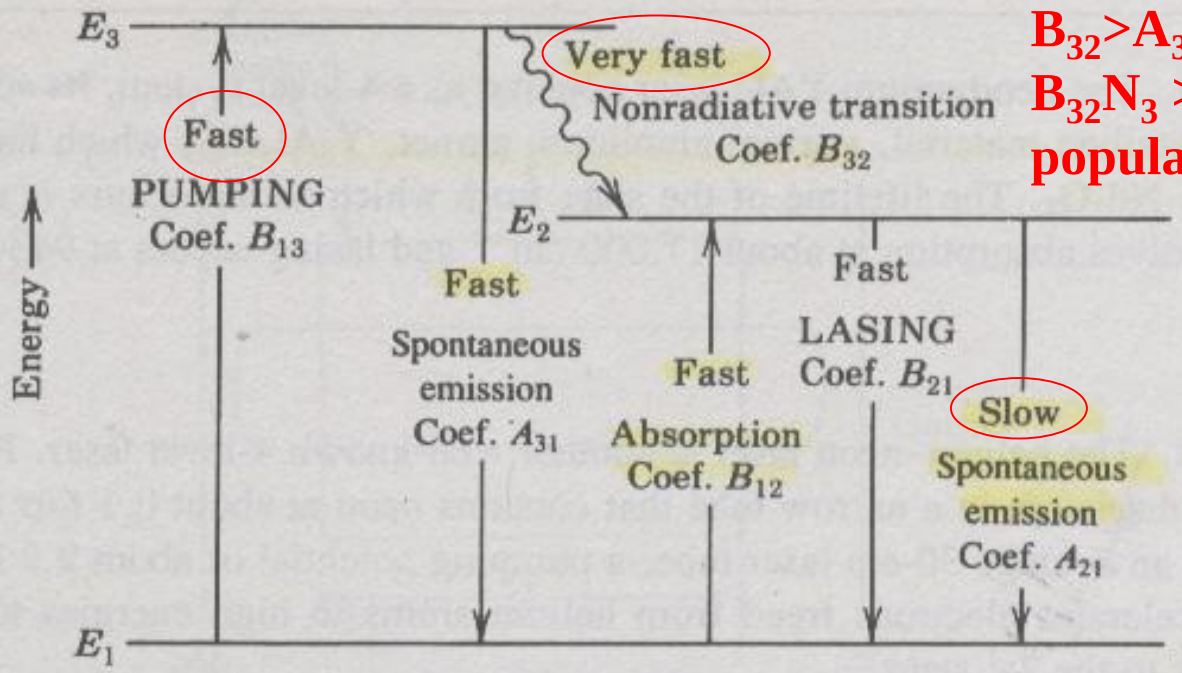

$B_{32} > A_{31}$

$B_{32}N_3 > A_{21}N_2$: population inversion

Fig. 8.7 A simplified three-level laser diagram. The system is pumped to excited state E_3 from ground state E_1 either by a flash lamp or an electric discharge. Relaxation from E_3 to E_2 occurs by a very rapid nonradiative reaction. Often the process is internal conversion between electronic states or vibrational relaxation within the excited electronic state. If $D_{32} > A_{31}$, most species will enter level E_2. Further, if $A_{21}N_2 < D_{32}N_3$, the population of E_2 may increase sufficiently to form a population inversion.

Four-Level Laser Systems

Fore-level system is much more efficient:
small expenditure of pumping energy

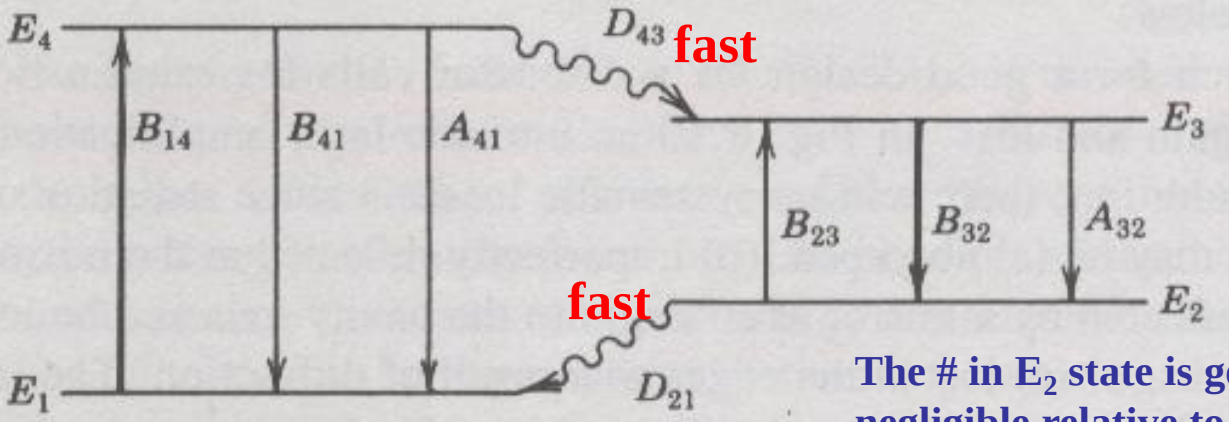

The # in E_2 state is generally negligible relative to # in E_1 & E_3 state

Fig. 8.9 A simplified four-level laser diagram. Pumping and lasing transitions are shown by heavy lines. Probability coefficient symbols are given for transitions. For kinetics to favor the buildup of population in level E_3, the lifetime E_3 should be relatively long and at least one fast mechanism should exist for relaxation from E_2. A nonradiative mechanism is suggested here.

Dye Laser

-The active materials in dye lasers are solutions of organic compounds capable of fluorescing in the UV, Vis or IR (Four level system)
- tunable over rage 20 to 50 nm, bandwidth < a few hundredth of nanometer

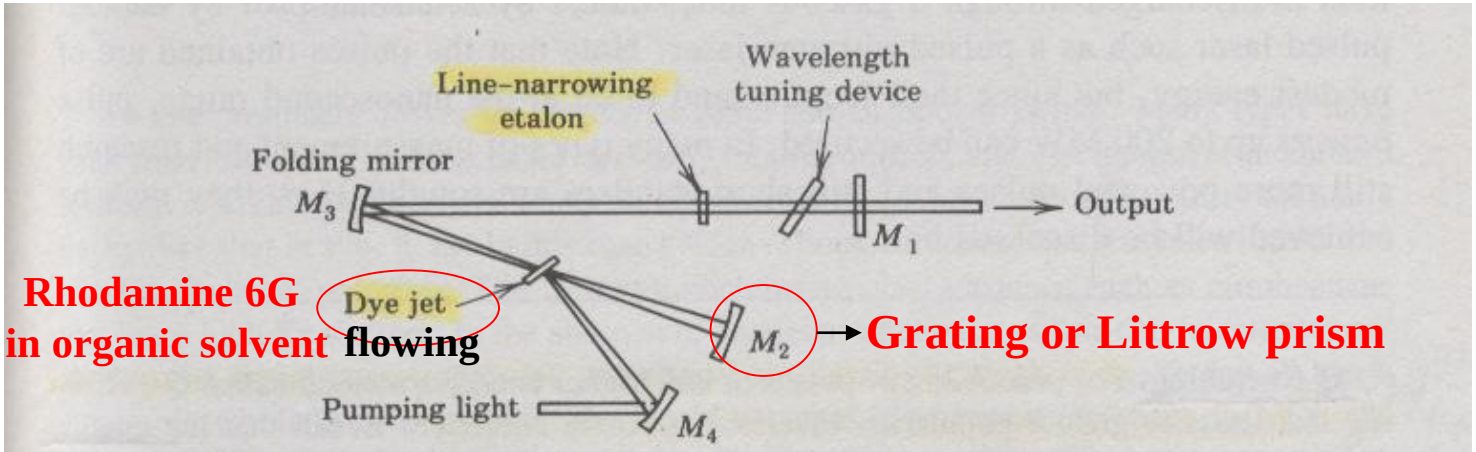

Fig. 8.13 Simplified diagram of a representative continuous-v
extends from mirror M_2 (totally reflecting) to mirror M_1. The la
coupler since it has a transmittance of about 0.03. This reson
curvature of mirrors M_2 and M_3 is chosen to give a beam waist a
of the dye stream. The dye jet is at the Brewster angle with resp
laser cavity is essentially stigmatic. The steady flow of dye rec
pumping. The pumping radiation from an Ar ion or N_2 laser (nc
mirror M_4. An etalon whose thickness is just over half $\frac{1}{2}\Delta\nu_R$,
band, is often inserted as a line-narrowing or mode-locking de
packet of perhaps three birefringent plates is rotated (or a tapered
in the cavity beam.

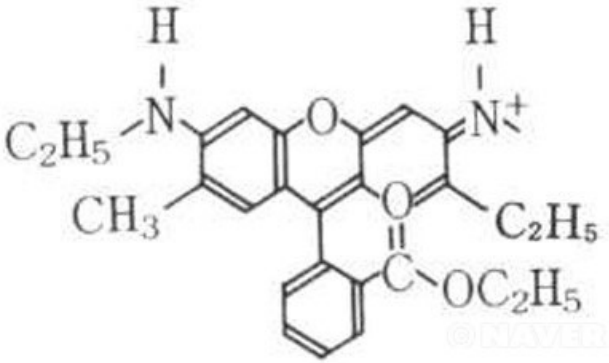

Semiconductor Diode (Light Emitting Diode)

E_g: band gap energy between valence band and conduction band

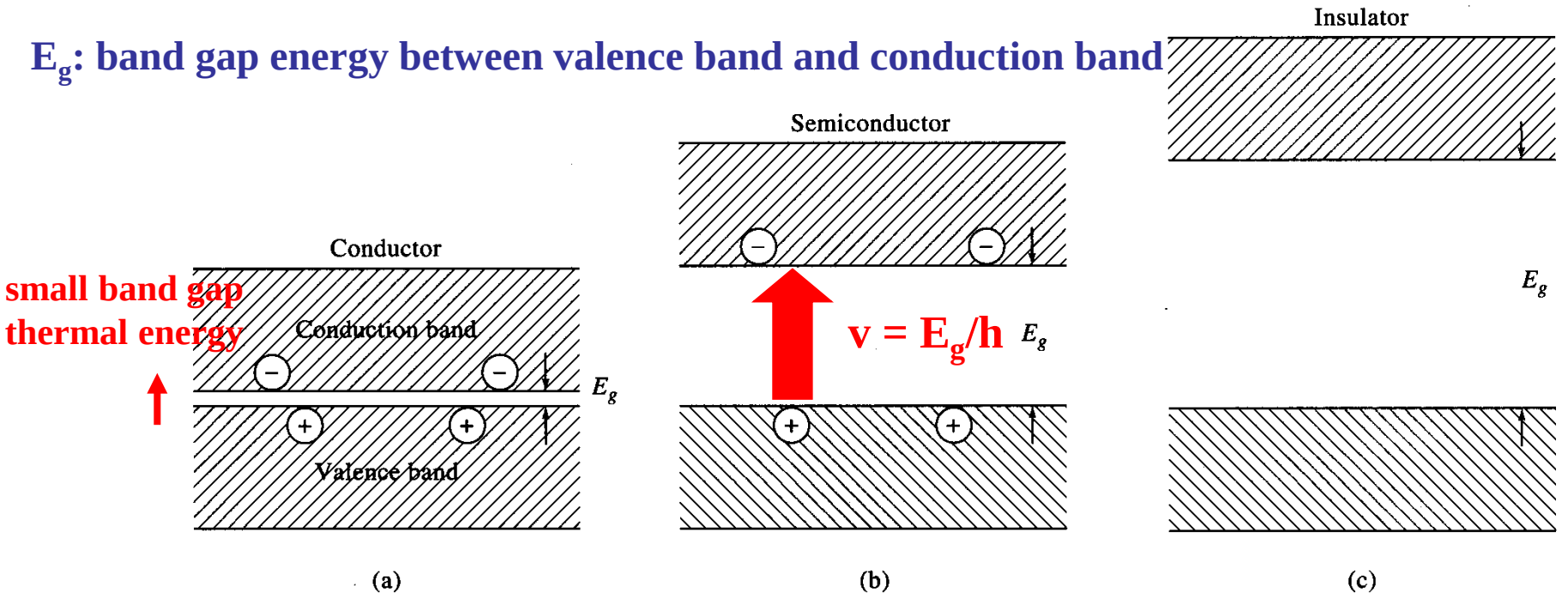

Figure 7-8 Conduction bands and valence bands in three types of materials.

(1) A voltage is applied across a semiconductor diode in a forward direction (excitation).
(2) Some of the electrons relax and emit radiation.
(3) Light emitting diode (LED): GaAs doped with P (660 nm)
(4) Limited utility in spectroscopy: low intensity & limited λ.

Anal. Chem. **2007**, *79*, 7005−7013

Identification of Inorganic Improvised Explosive Devices by Analysis of Postblast Residues Using Portable Capillary Electrophoresis Instrumentation and Indirect Photometric Detection with a Light-Emitting Diode

Joseph P. Hutchinson, Christopher J. Evenhuis, Cameron Johns, Artaches A. Kazarian, Michael C. Breadmore, Miroslav Macka,† Emily F. Hilder, Rosanne M. Guijt, Greg W. Dicinoski, and Paul R. Haddad*

Australian Centre for Research on Separation Science (ACROSS), School of Chemistry, Faculty of Science, Enginee and Technology, University of Tasmania, Private Bag 75, Hobart, Tasmania, 7001, Australia

Table 2. Analytical Figures of Merit for Cation Separation System by CE

analyte	retention time ($n = 10$) min	retention time ($n = 10$) RSD (%)	peak area RSD (%)	theoretical plates/m	resolution	LOD (S/N = 3, mg/L)	calibration R^2
1 monomethylammonium	2.388	1.03	8.55	89 000	3.16	0.21	0.9925
2 ammonium	2.545	1.08	10.7	97 000	1.04	0.20	0.9906
3 ethylammonium	2.583	1.02	9.02	134 000	3.26	0.19	0.9882
4 potassium	2.724	0.91	16.1	103 000	6.25	0.22	0.9889
5 sodium	3.074	0.96	10.6	84 000	11.8	0.11	0.9867
6 barium	4.123	0.83	17.5	75 000	3.11	1.26	0.9869
7 strontium	4.462	0.72	11.8	100 000	2.76	0.57	0.9834
8 magnesium	4.745	0.93	11.6	71 000	1.38	0.13	0.9858
9 calcium	4.889	0.77	16.5	99 000	5.47	0.23	0.9898
10 manganese	5.432	0.94	13.3	120 000	19.3	0.37	0.9828
11 zinc	8.425	0.70	11.6	93 000	1.30	0.52	0.9823
12 lead	8.669	0.92	12.3	84 000		2.30	0.9847

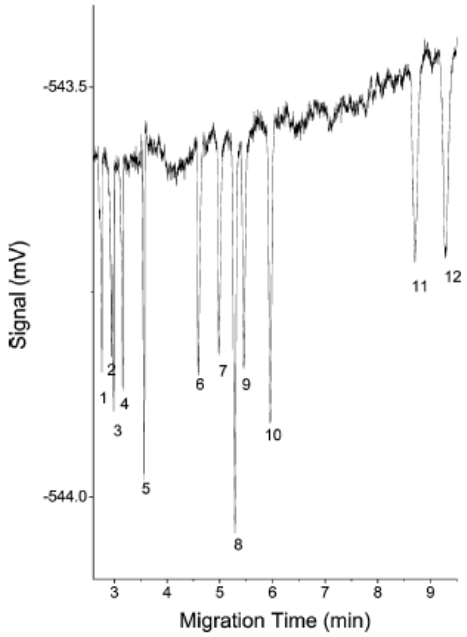

Figure 2. CE separation of target cation mixture using the portable CE-P2 equipped with a miniaturized indirect photometric LED detector. Conditions: 75-μm-i.d. fused-silica capillary, $L_{total} = 55.5$ cm. BGE was 10 mM chrysoidine in MeOH, with 0.7% glacial acetic acid added. Separation voltage, 25 kV. Detection performed using a 470-nm LED source, operating current 40 mA, 9.5 cm from cathode ($L_{detector} = 46.0$ cm). An extended UV photodiode detector collected the signal obtained. Samples injected using a pressure of 0.1 psi for 1 s. Sample concentrations: 20.5 mg/L ammonium, 41 mg/L methylammonium, ethylammonium, potassium, sodium, magnesium, and calcium, 81.5 mg/L strontium, manganese, and zinc, 163 mg/L barium, and 326.5 mg/L lead. Cations are numbered throughout all figures in correspondence with Table 2.

Wavelength Selector

Components of Optical Spectroscopy

Wavelength Selector

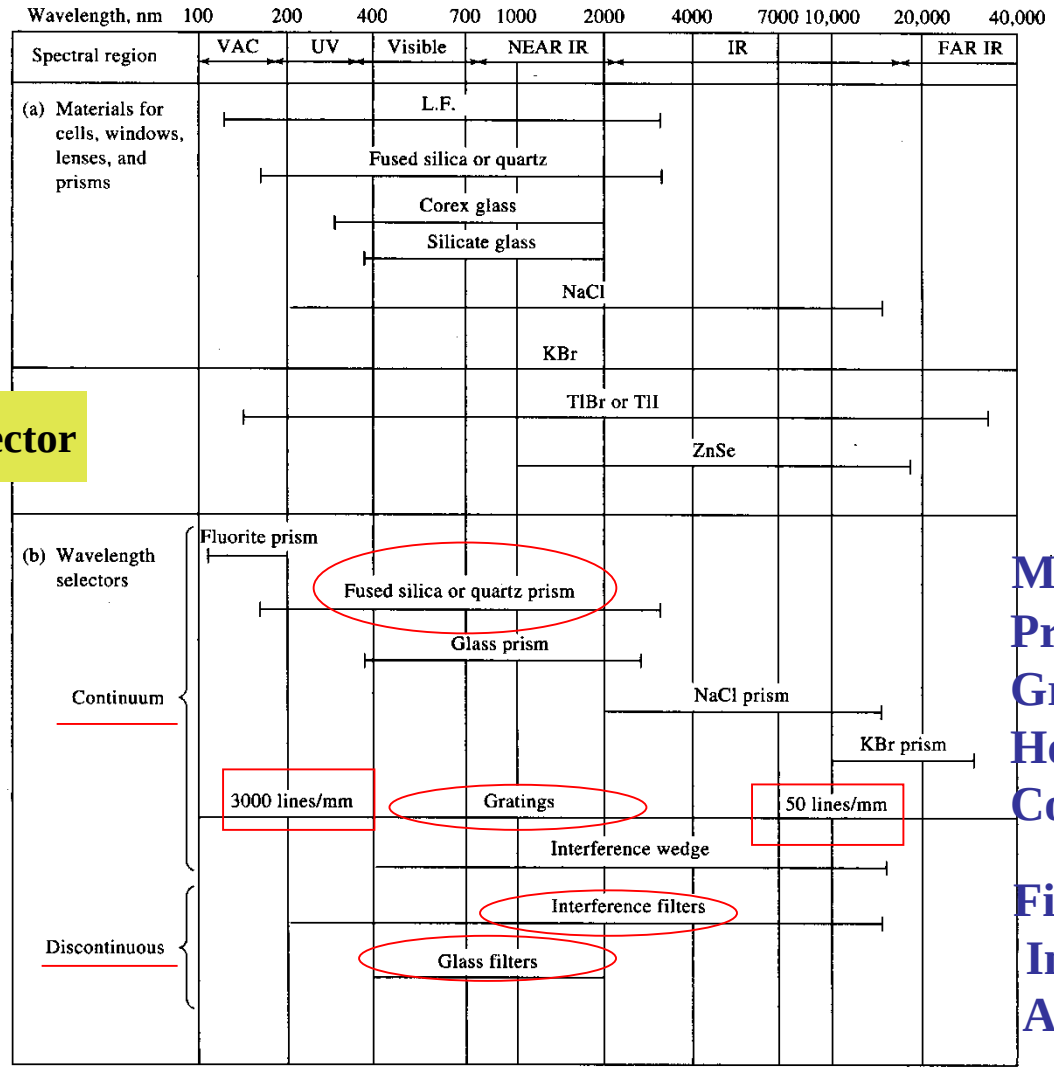

Figure 7-2 (a) Construction materials and (b) wavelength selectors for spectroscopic instruments.

Monochromators:
Prism M
Grating M
Holographic M
Concave M

Filters:
Interference F (UV-Vis, IR
Absorption F (Vis)

<Narrow bandwidth>

- Enhance **sensitivity** in absorbance measurements
- Enhance **selectivity** in absorption and emission methods

Ideal wavelength selector: provides an output of a single wavelength

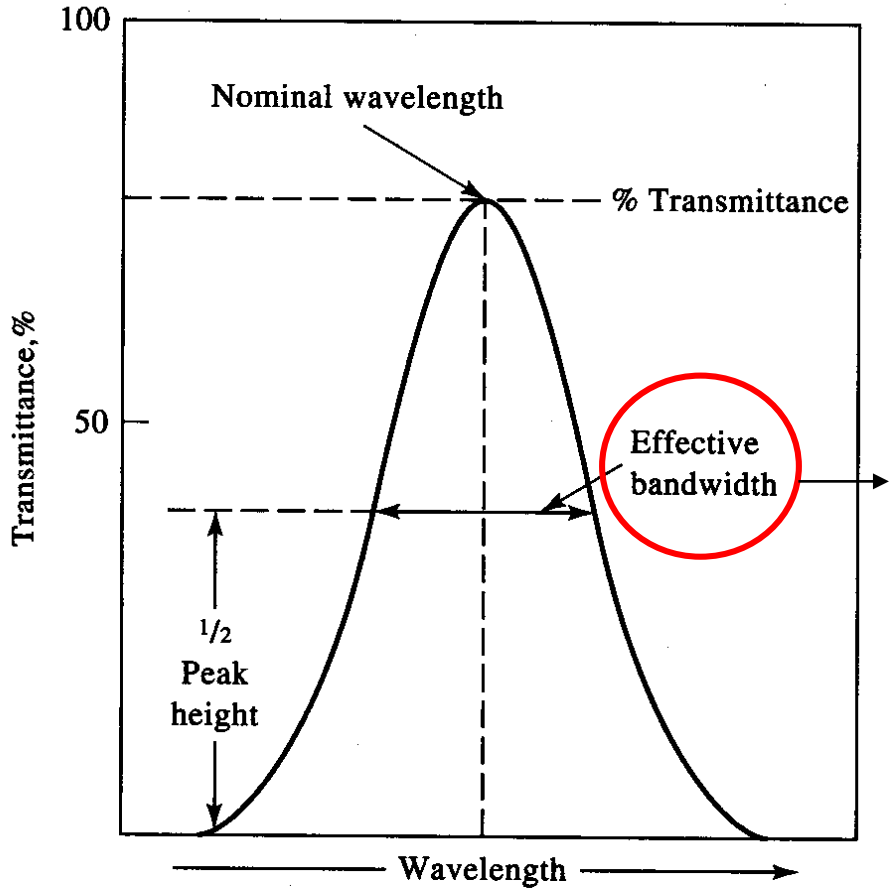

An inverse measure of the quality of the wavelength selector

Figure 7-11 Output of a typical wavelength selector.

Interference Filters (Fabry-Perot filters)

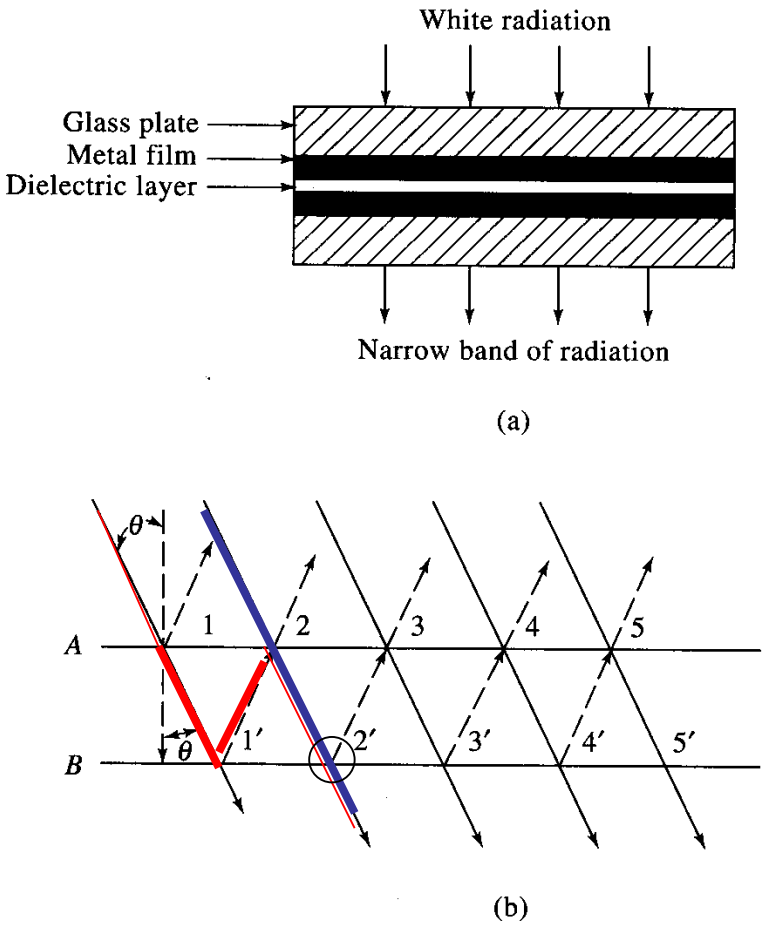

Figure 7-12 (a) Schematic cross section of an interference filter. Note that the drawing is not to scale and that the three central bands are much narrower than shown. (b) Schematic to show the conditions for constructive interference.

$n\lambda' = 2a$ (경로차)
constructive interference

$\lambda = 2\,t\,\eta/n$

λ: wavelength of transmitted radiation
t: thickness of dielectric material
η: refractive index of dielectric material

Interference Filters (Fabry-Perot filters)

- Available throughout UV, Vis, and IR region.
- Effective bandwidths are about 1.5% of the wavelength at peak transmittanc

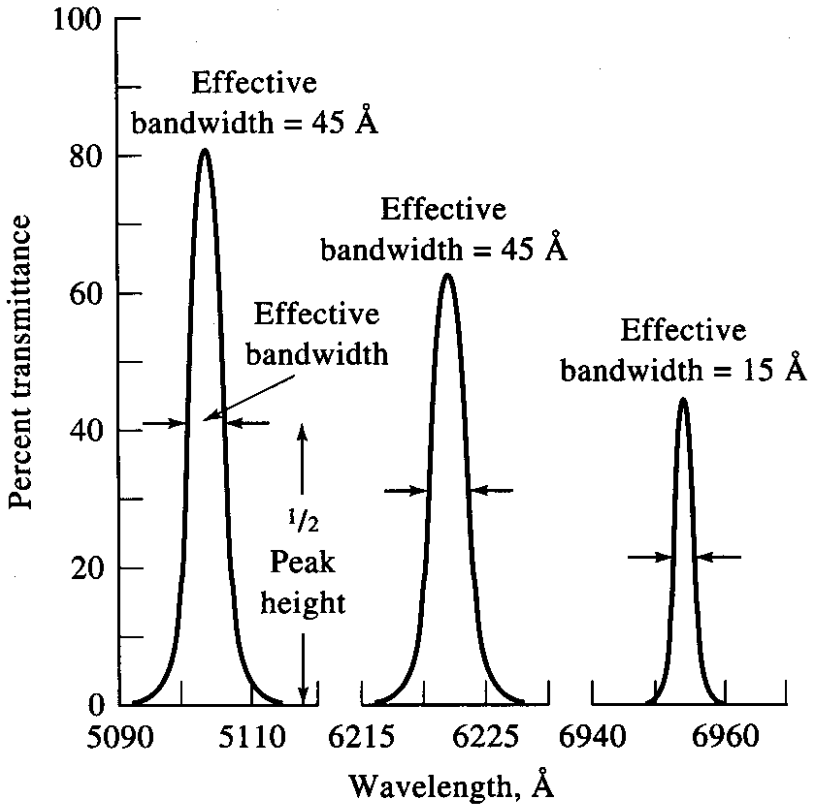

Figure 7-13 Transmission characteristics of typical interference filters.

Absorption Filters

- Absorbs certain portion of spectrum
- Consists of colored glass or of a dye suspended in gelatin
- Restrictedly used in the visible region
- Wide bandwidth (30-250 nm) and low transmittance (~10%)

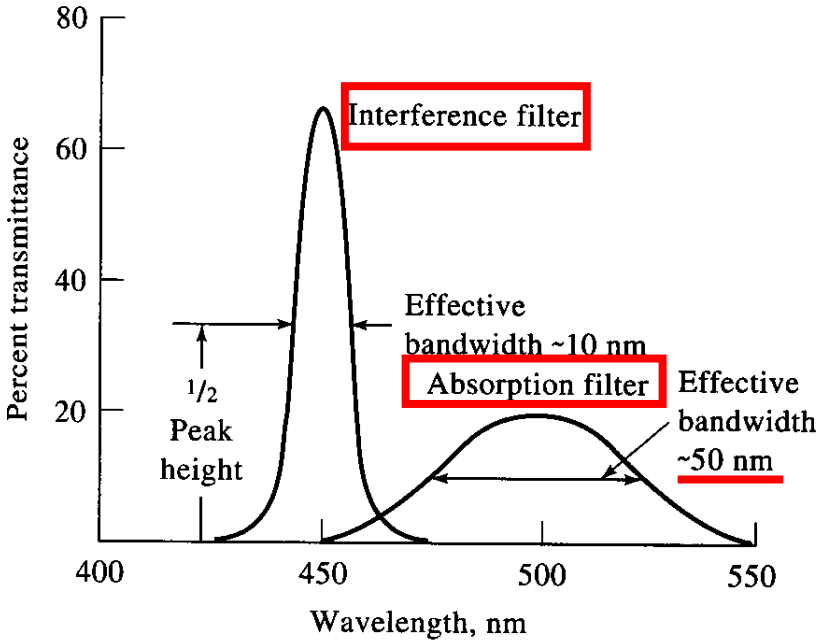

Figure 7-14 Effective bandwidths for two types of filters

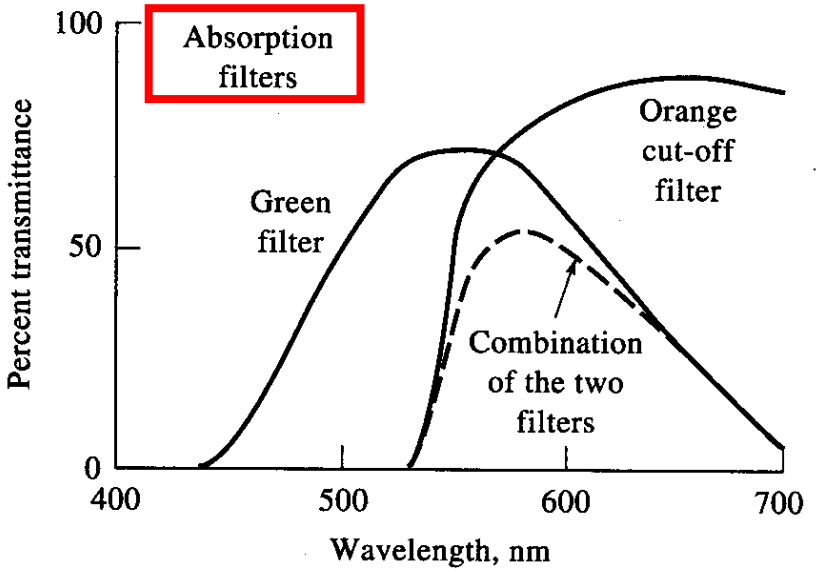

Figure 7-15 Comparison of various types of filters for visible radiation.

Photometer

Simple, relatively inexpensive tools for performing absorption analyses

Single-beam

Double-beam

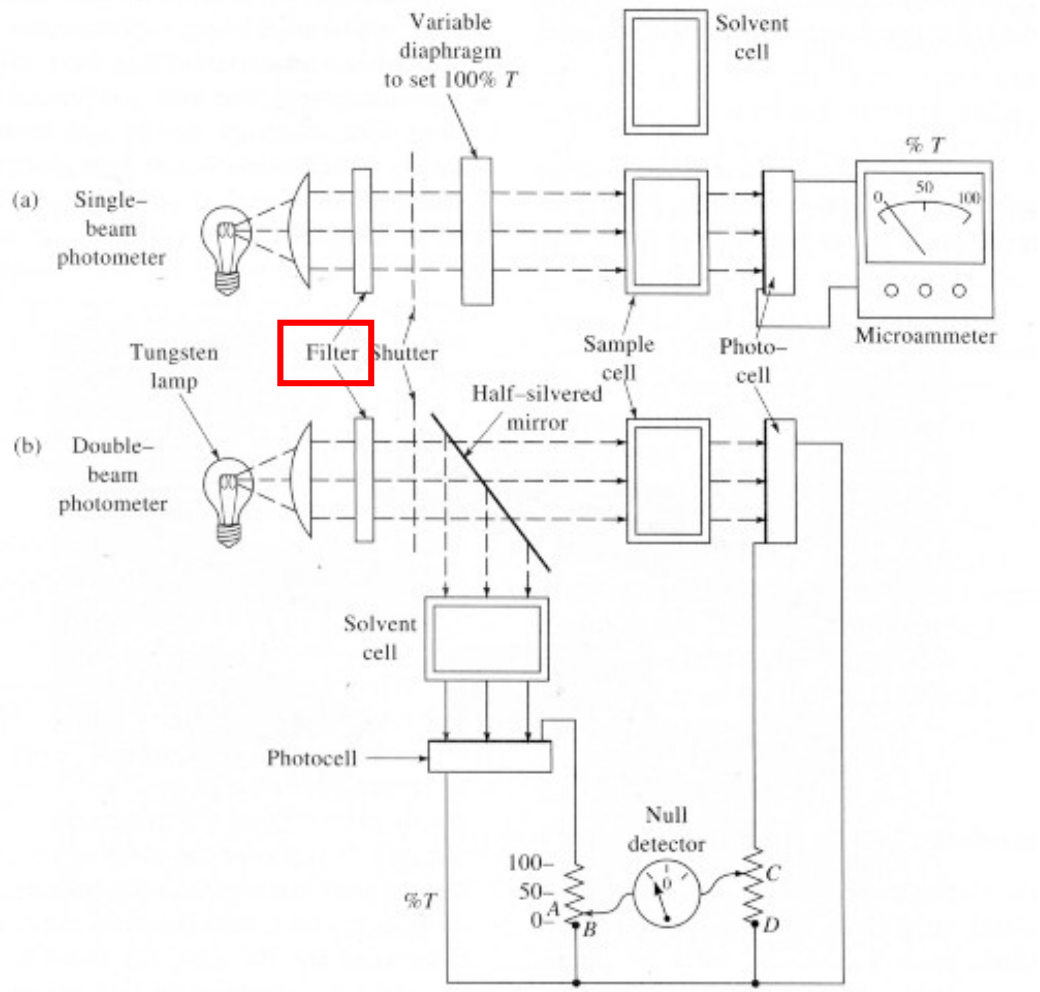

Figure 13-15 A single- and double-beam photometer.

Monochromators

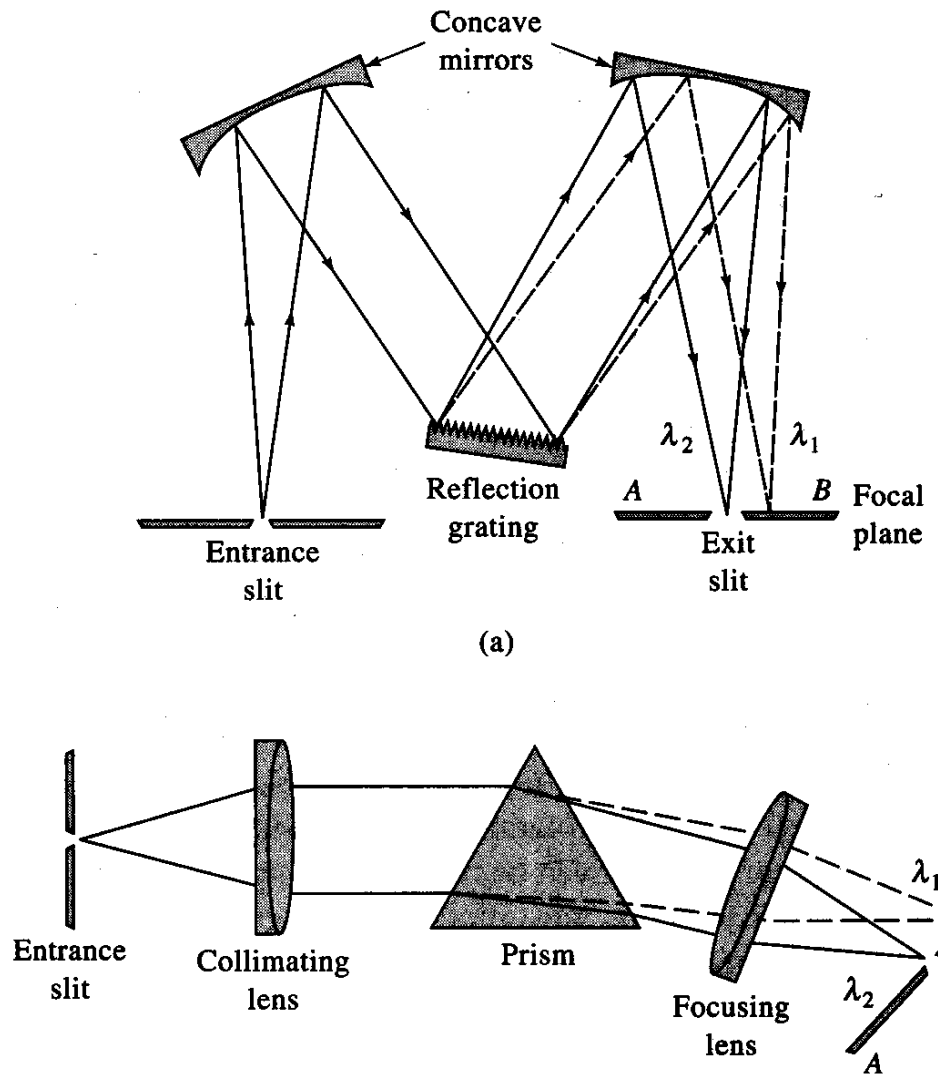

Figure 7-16 Two types of monochromators: (a) Czerney-Turner grating monochromator and (b) Bunsen prism monochromator. (In both instances, $\lambda_1 > \lambda_2$.)

1) Entrance slit that provides a narrow optical image
2) Collimator (mirror) that renders the rays spreading from the slit parallel
3) A component for dispersing this radiation
4) A focusing element to reform images of the slit
5) Exit slit to isolate the desired spectral band

Prism Monochromator

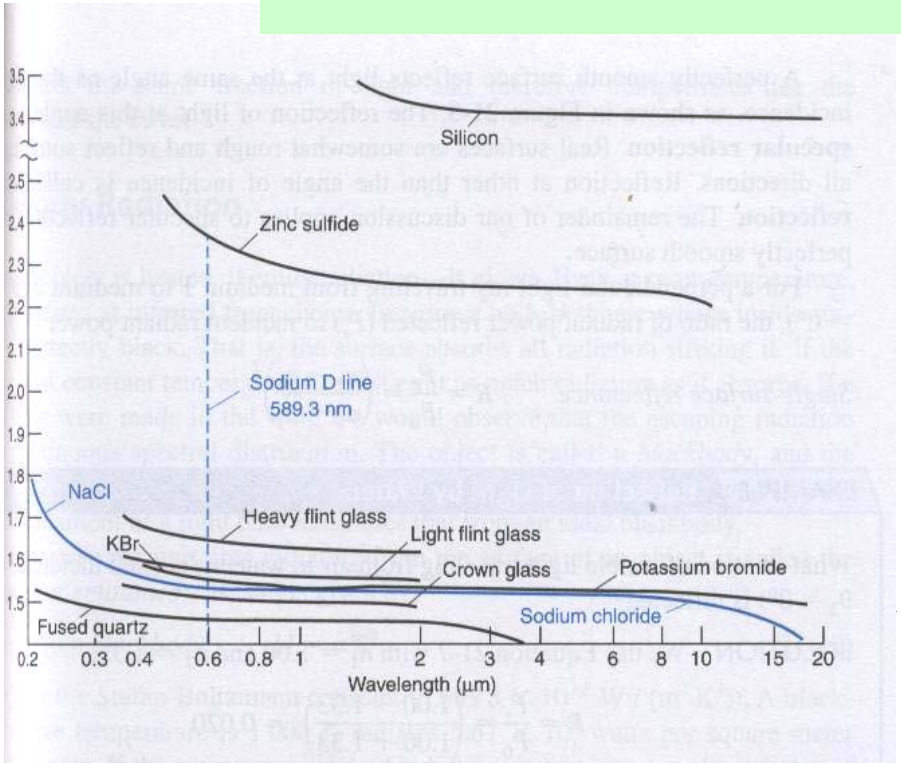

Different λ
→ different refractive index (n_2)
→ ($n_1 \sin\theta_1 = n_2 \sin\theta_2$), ($n_1$, θ_1 the same)
→different refractive angle (θ_2)
→ different focal position

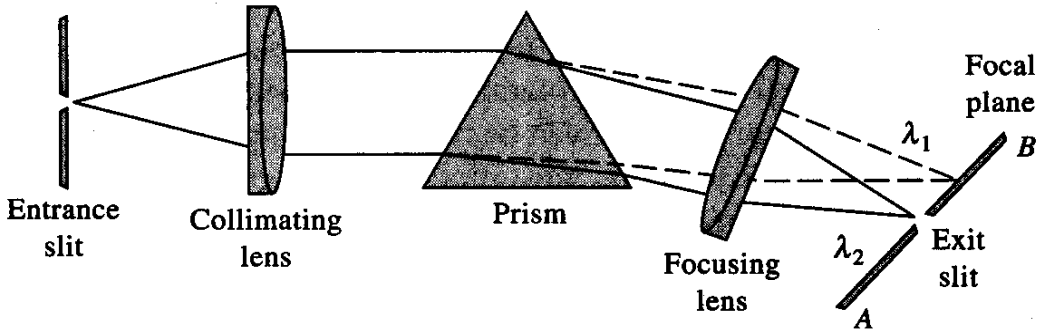

(b)

λ2 < λ1

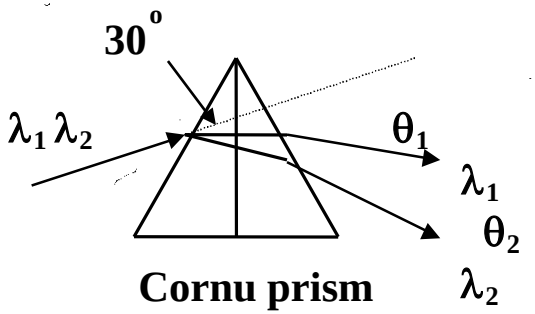

Cornu prism

Prism Monochromator

Transmittance prism: Cornu
Reflection prism: Littrow

Reflection occurs

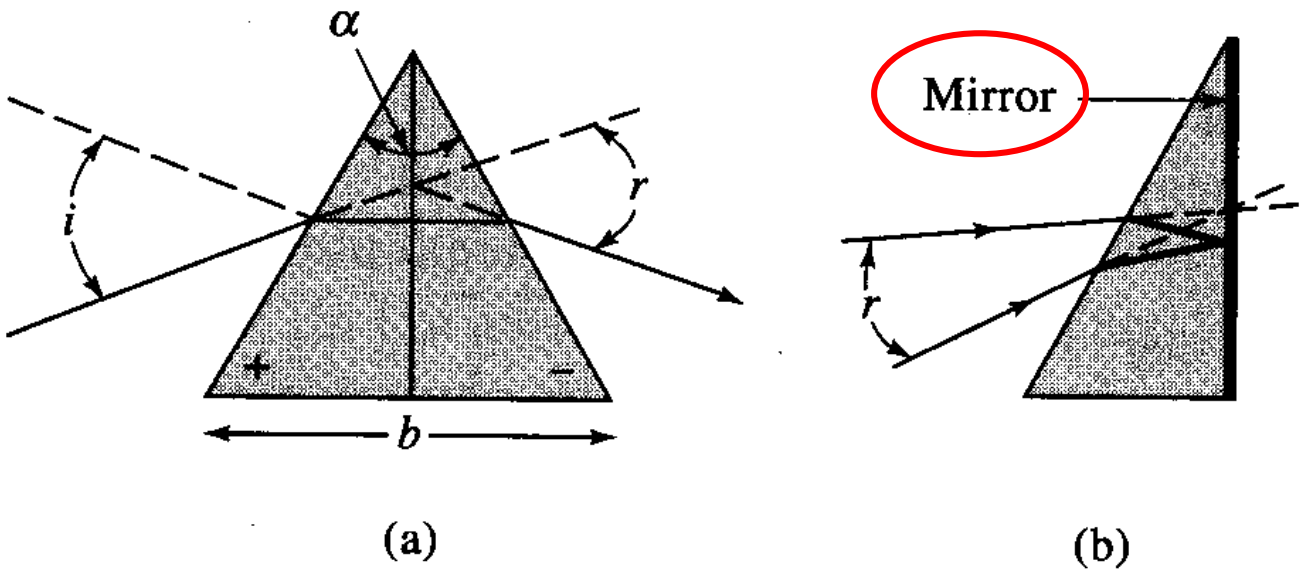

Figure 7-18 Dispersion by a prism: (a) quartz Cornu types and (b) Littrow type.

Grating : Echellette-Type

Beam 1 and Beam 2의 경로차: $\overline{CB} + \overline{BD}$

Constructive interference:

$$n\lambda = \overline{CB} + \overline{BD} = d \sin i + d \sin r = d (\sin i + \sin r)$$

i: incidence angle, r: reflection (diffraction) angle, n: diffraction order, d: groove distance

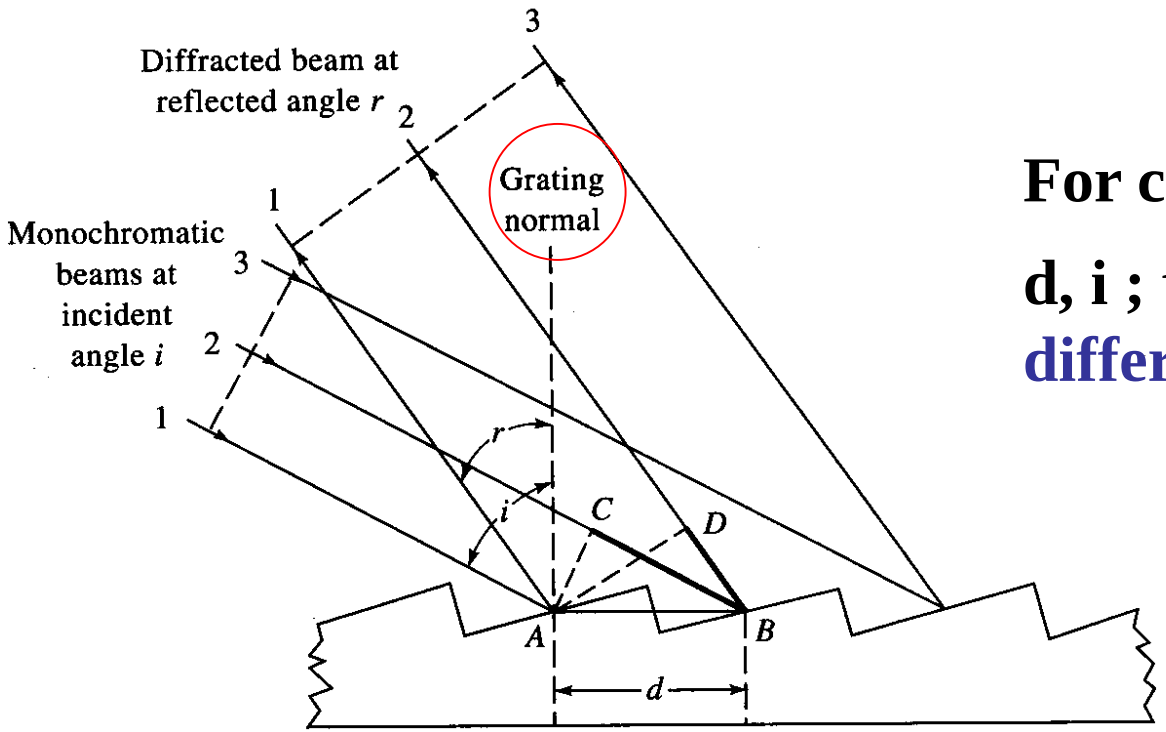

Figure 7-19 Mechanisms of diffraction from an echellette-type grating.

For constructive interference

d, i ; the same for all λ

different λ → different r

Example:

1 mm당 1450개의 홈을 가지고 있는 echellette 회절발에 법선에 대하여 48°의 입사각으로 다색광을 비추었다. 반사각 +20, +10, 0도에서 나타나는 복사선의 파장을 계산하여라.

d = (1mm/1450개의 홈) * 10^6nm/mm = 689.7 nm/홈

r = 20 ° λ = (698.7 / n) (sin 48 + sin 20) = 748.4 / n

r, 각도	n = 1	n = 2	n = 3
0	513	256	171
10	632	316	211
20	748	374	249
30	858	429	286
40	956	478	318
50	1040	520	346
60			
70	1161	580	387
80			
90	1202	601	400

most intense **high order lines are removed by filters**

Grating : Transmission

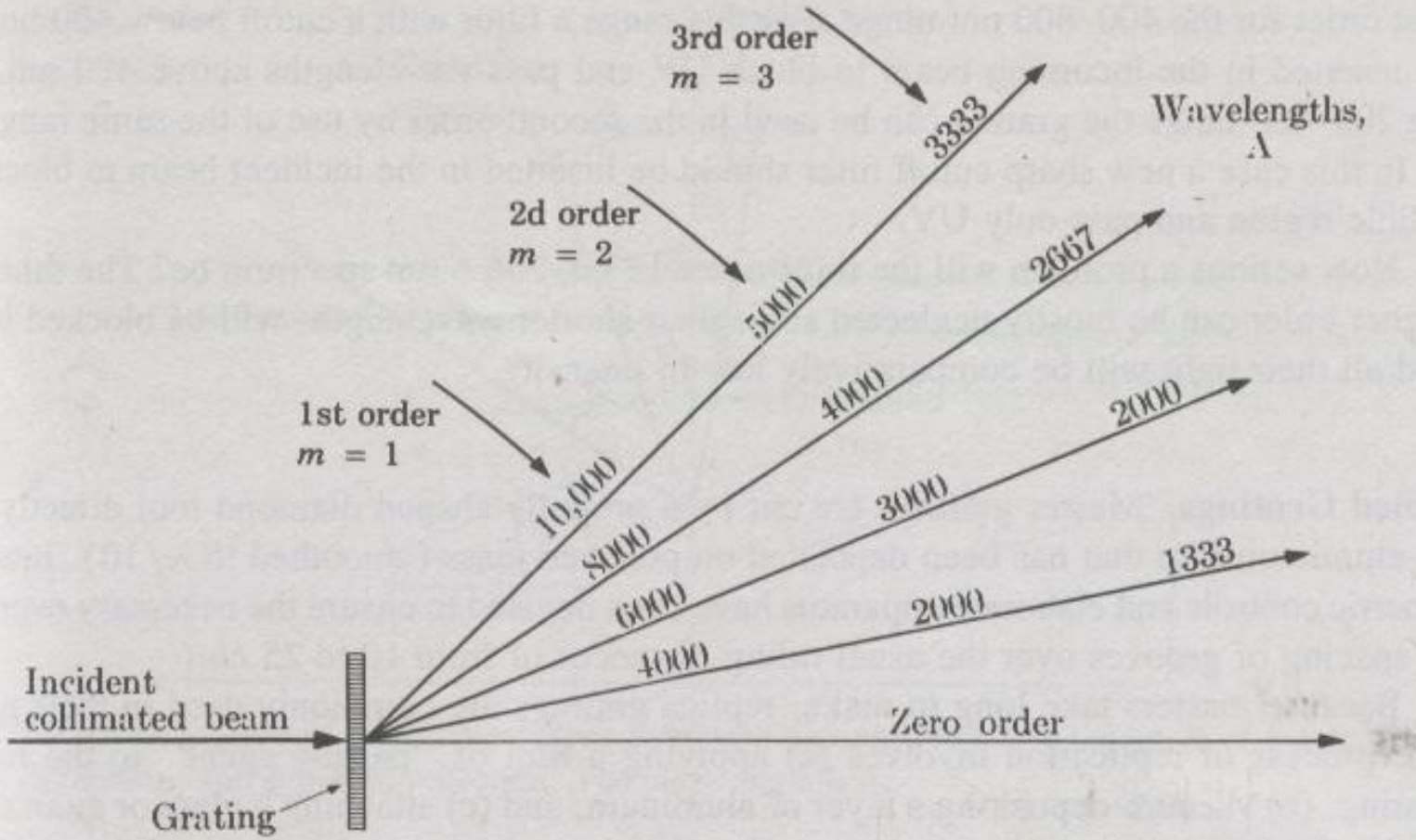

Fig. 9.13 Overlapping orders of spectra from transmission grating. A similar set of orders is formed at equal angles below the normal.

Resolution in Monochromator

The limit of its ability to separate closely spaced peaks that have a slight difference in wavelength.

$$R = \frac{\lambda}{\Delta\lambda} = nN$$

λ: average wavelength of the two peaks
$\Delta\lambda$: difference
n: diffraction order
N: number of grooves of the grating illuminated by radiation from entrance slit

Better resolution:

- higher N
- higher diffraction order

Grating : Echelle-Type

- **The blaze angle of an echelle grating is significantly higher than the echellette**
- **The short side of the blaze is used rather than the long**
- **The grating is relatively coarse: ~ 300/mm (1200-1400/mm, conventional type)**
- **The angle of reflection *r* is much higher in echelle than in echellette.**
- **$r = i = \beta$, $n\lambda = 2d \sin\beta$**

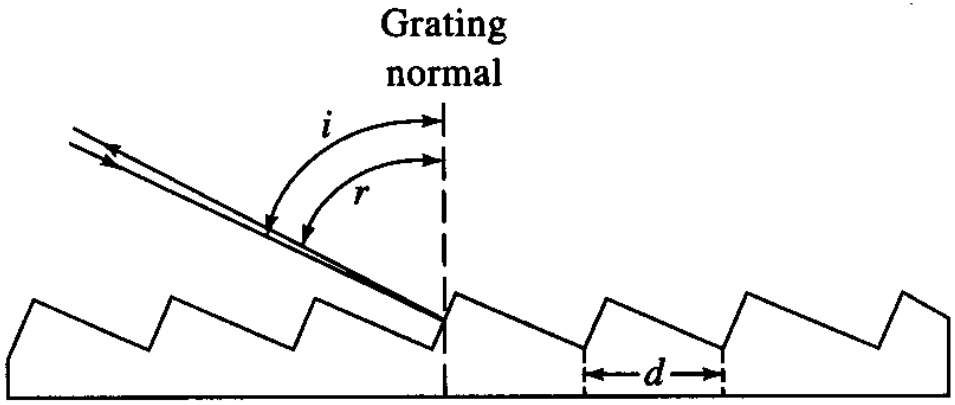

Figure 7-20 Echelle grating: i = angle of incidence; r = angle of reflection; d = groove spacing. In usual practice, $i \approx r = \beta = 63°26'$.

Echelle Monochromator

Two dispersion elements arranged in series : higher dispersion and resolution than an echellette of the same size

Used in atomic emission spectroscopy

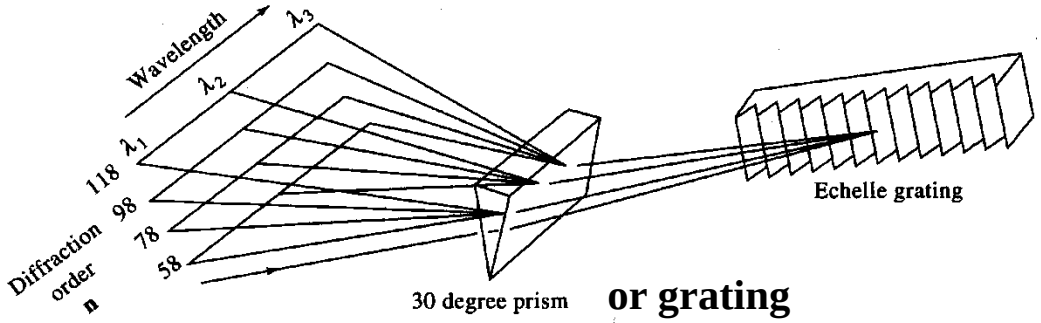

or grating (low dispersion)

(a)

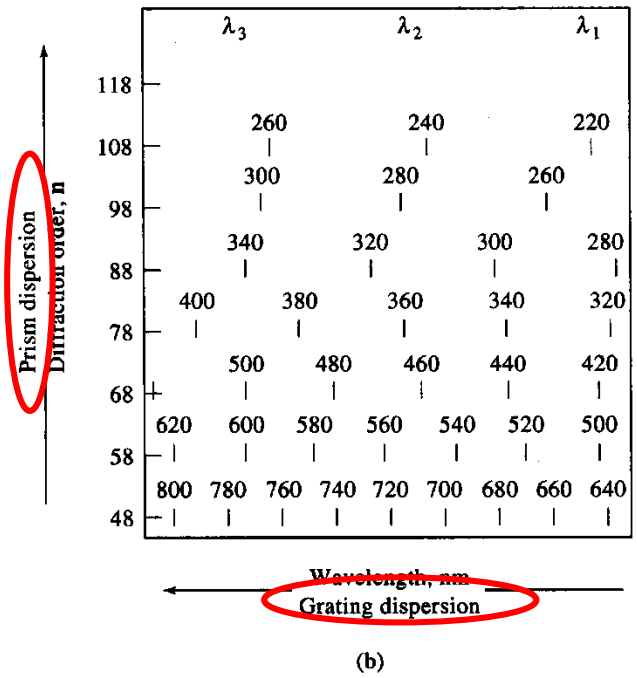

(b)

Figure 7-21 An echelle monochromator: (a) arrangement of dispersing elements, and (b) schematic end-on view of the dispersed radiation from the point of view of the transducer.

Echelle Monochromator in AES

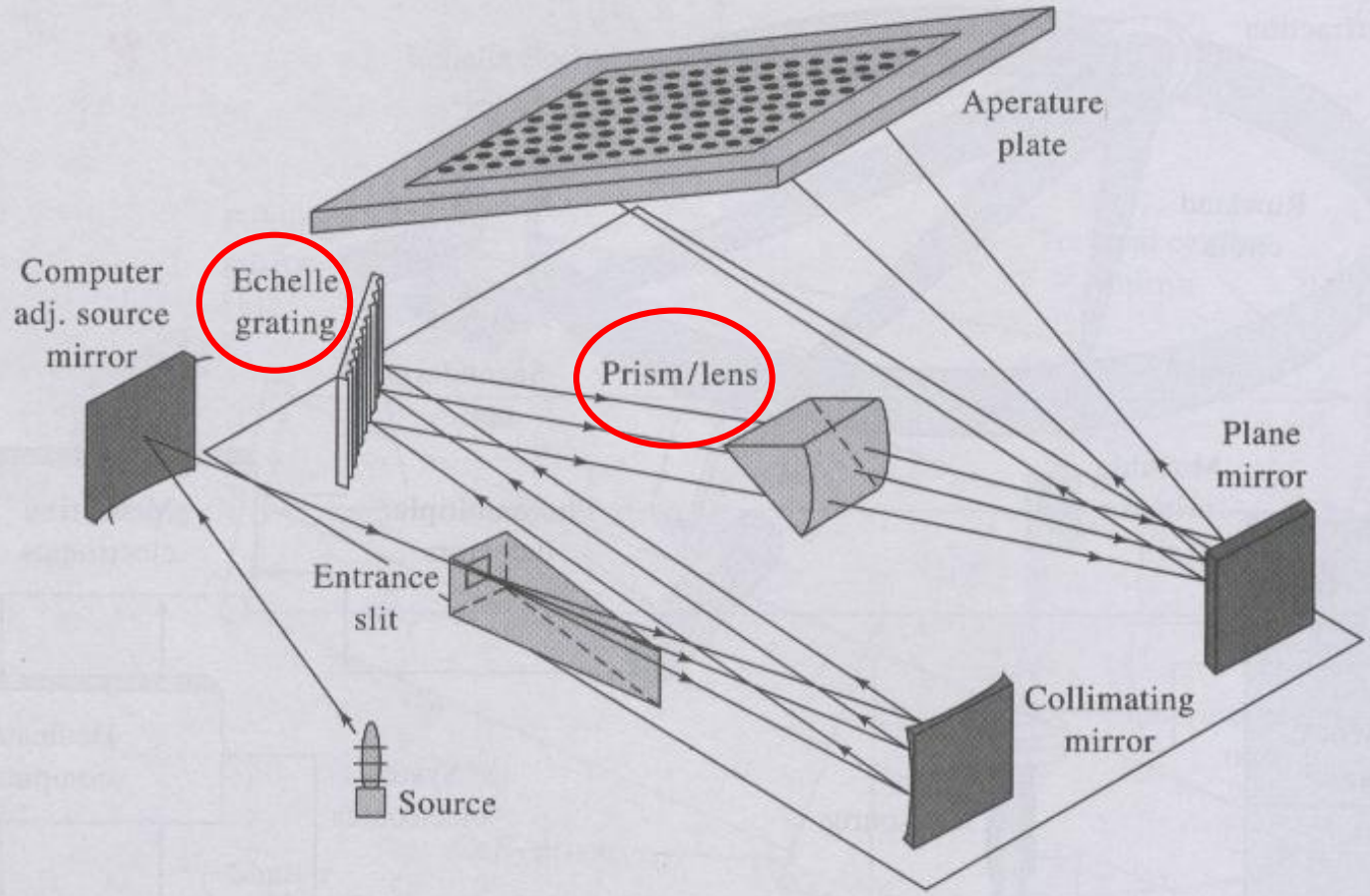

Figure 10-7 Schematic of an echelle polychromator system.

Polychromator

In polychromator, diffraction grating is locked in place, the exit slit is removed, and a multi-channel detector is permanently installed along the focal plane.

High speed and wavelength accuracy

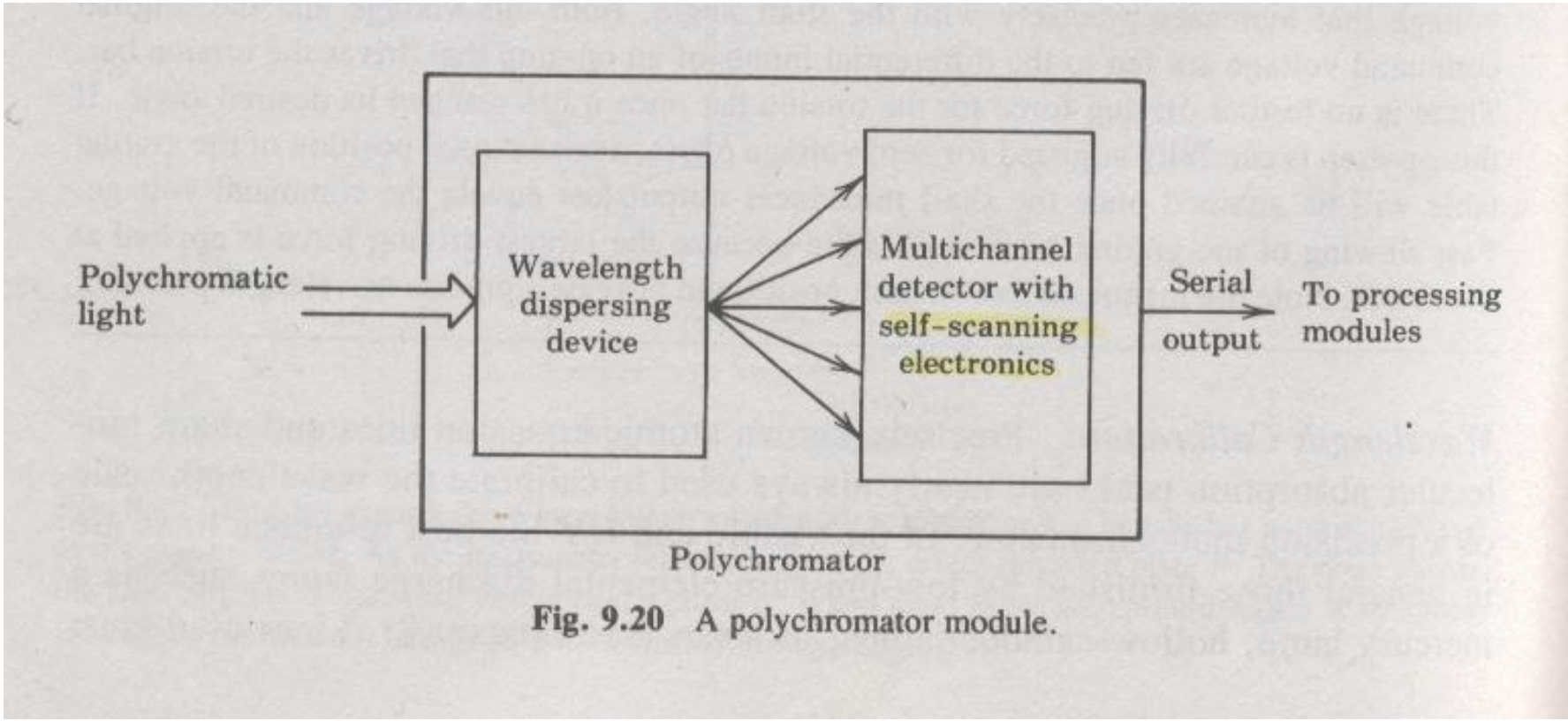

Fig. 9.20 A polychromator module.

Effect of Slit Width

A narrow slit will optimize resolution, while wide one will optimize energy

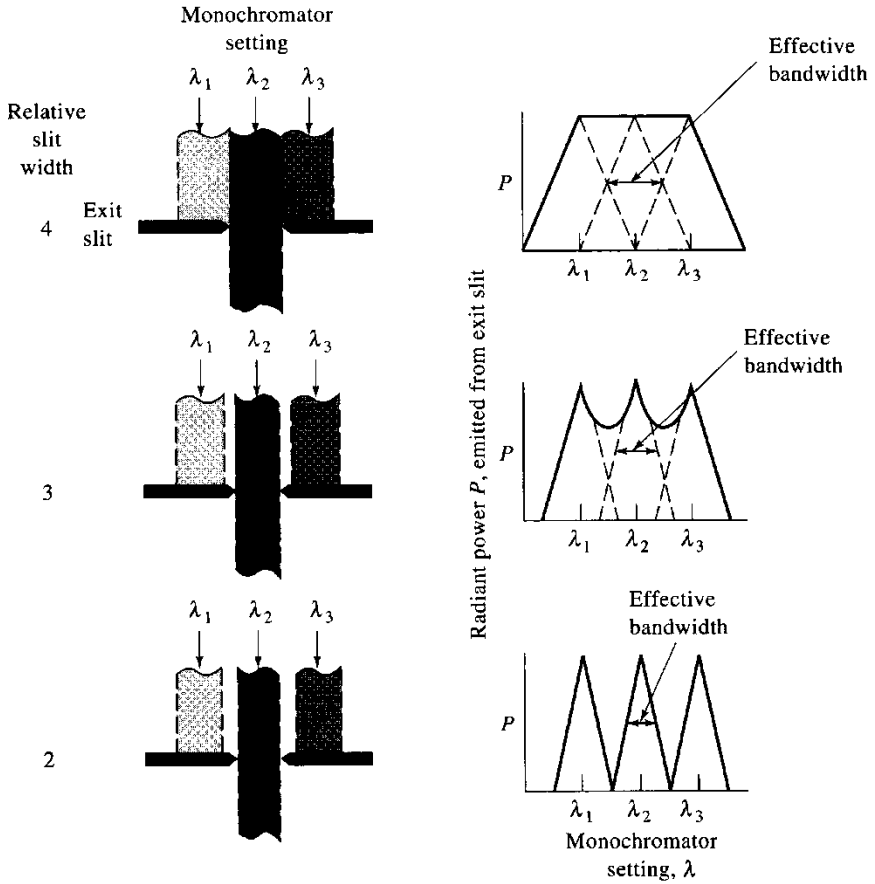

Figure 7-23 The effect of the slit width on spectra. The entrance slit is illuminated with λ_1, λ_2, and λ_3 only. Entrance and exit slits are identical. Plots on the right show changes in emitted power as the setting of monochromator is varied.

Better resolution
Lower power

Qualitative analysis: narrow slit width, Quantitative analysis: wide slit width

Effect of Slit Width

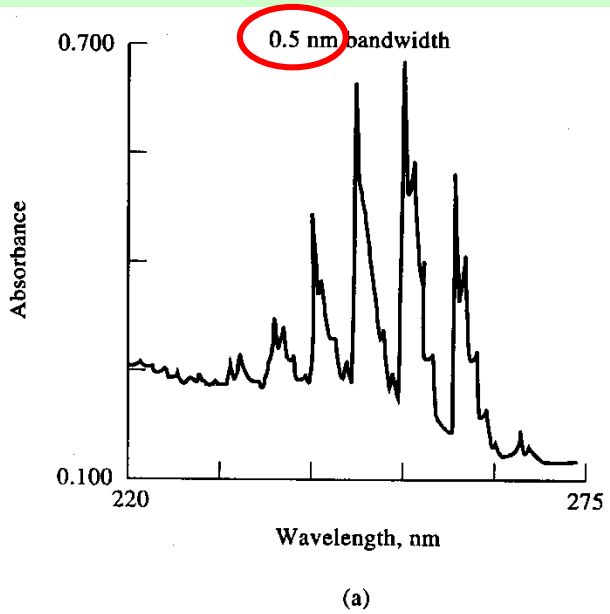

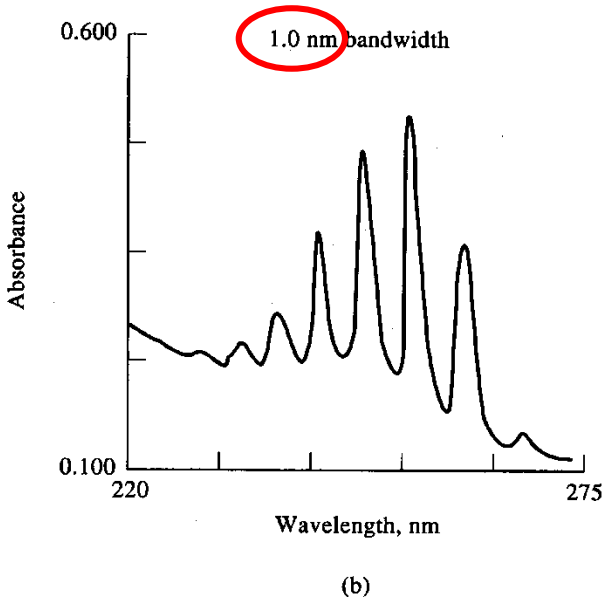

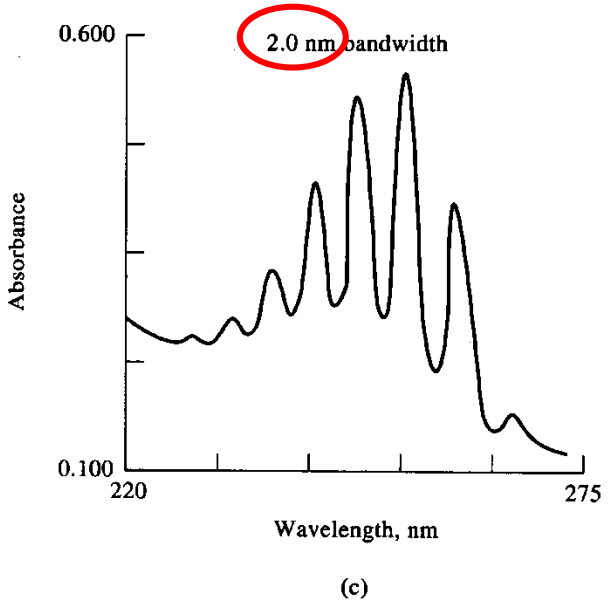

The much greater spectral detail can be realized with the narrowest slit setting

Figure 7-24 Effect of bandwidth on spectral detail for benzene vapor: (a) 0.5 nm; (b) 1.0 nm; (c) 2.0 nm. *(From V. A. Kohler,* Amer. Lab., ***1984*** *(11), 132. Copyright 1984 International Scientific Communications Inc.)*

Detector

Components of Optical Spectroscopy

Light Detector

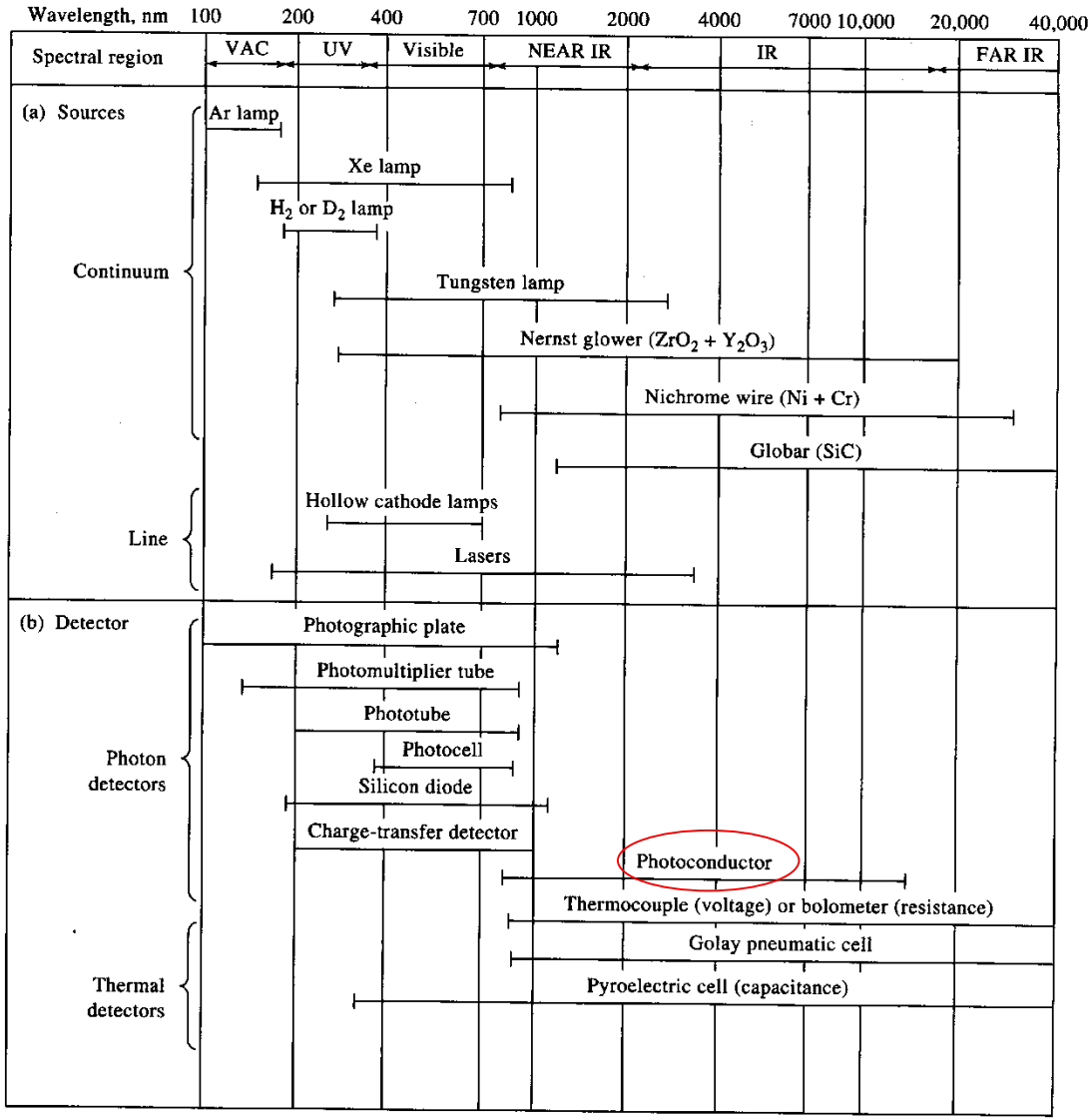

Figure 7-3 (a) Sources and (b) detectors for spectroscopic instruments.

Spectral Response of Light Detector

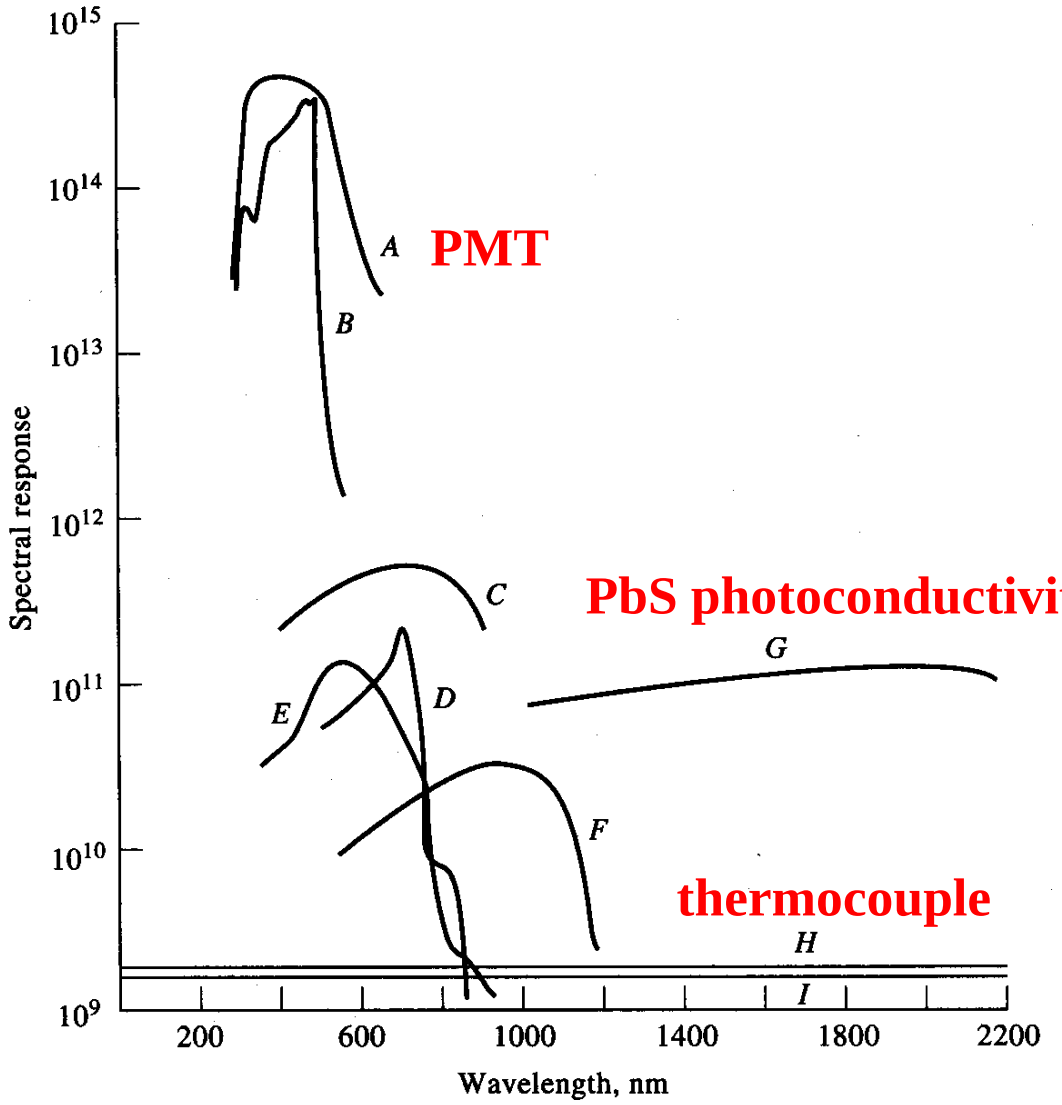

Figure 7-25 Relative response of various types of photoelectric transducers *(A–G)* and heat transducers *H, I*): *A,* photomultiplier tube; *B,* CdS photoconductivity; *C,* GaAs photovoltaic cell; *D,* CdSe photoconductivity cell; *E,* Se/SeO photovoltaic cell; *F,* silicon photodiode; *G,* PbS photoconductivity; *H,* thermocouple; *I,* Golay cell. *(Adapted from P. W. Druse, L. N. McGlauchlin, and R. B. Quistan,* Elements of Infrared Technology, *pp. 424–425. New York: Wiley, 1962. Reprinted by permission of John Wiley & Sons Inc.)*

Photomultiplier Tube (PMT)

- Good for the measurement of low radiation
- Photo-emissive surface (photocathode) + several dynodes
- Photocurrent is amplified: Gain of $10^6 - 10^9$
- Very stable power supply is required
- Highly sensitive to UV-VIS range
- Extremely fast response time
- Sensitivity is limited by dark current electrons

(thermal emission is major source)

: cooling is good for the enhancement of PMT performance → - 30 °C: no dark current

- PMT is limited to measuring low-power radiation (intense light causes irreversible damage to the photoelectric surfaces)

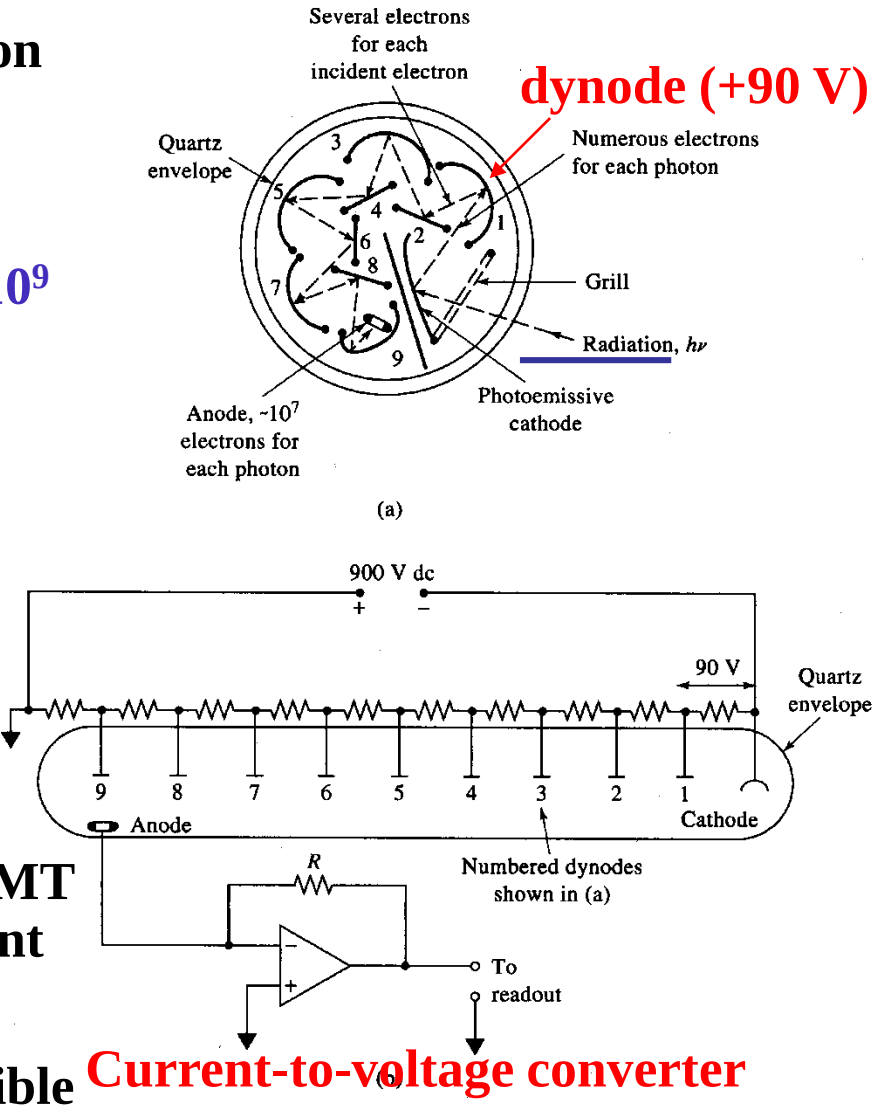

Figure 7-29 Photomultiplier tube: (a) cross-section of the tube and (b) electrical circuit.

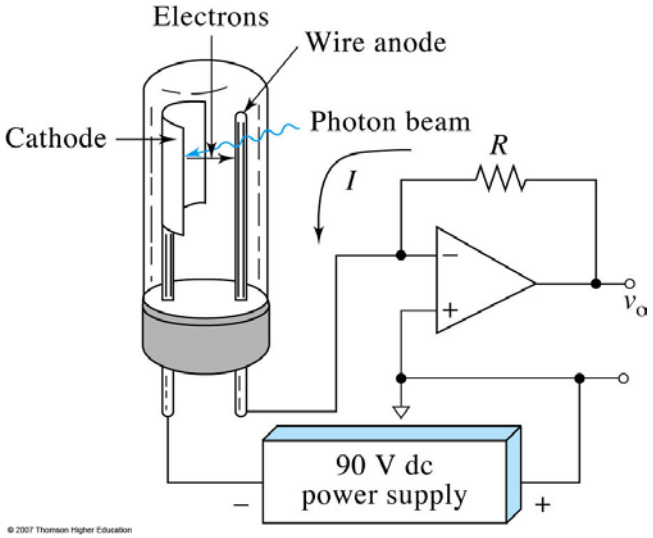

(a)

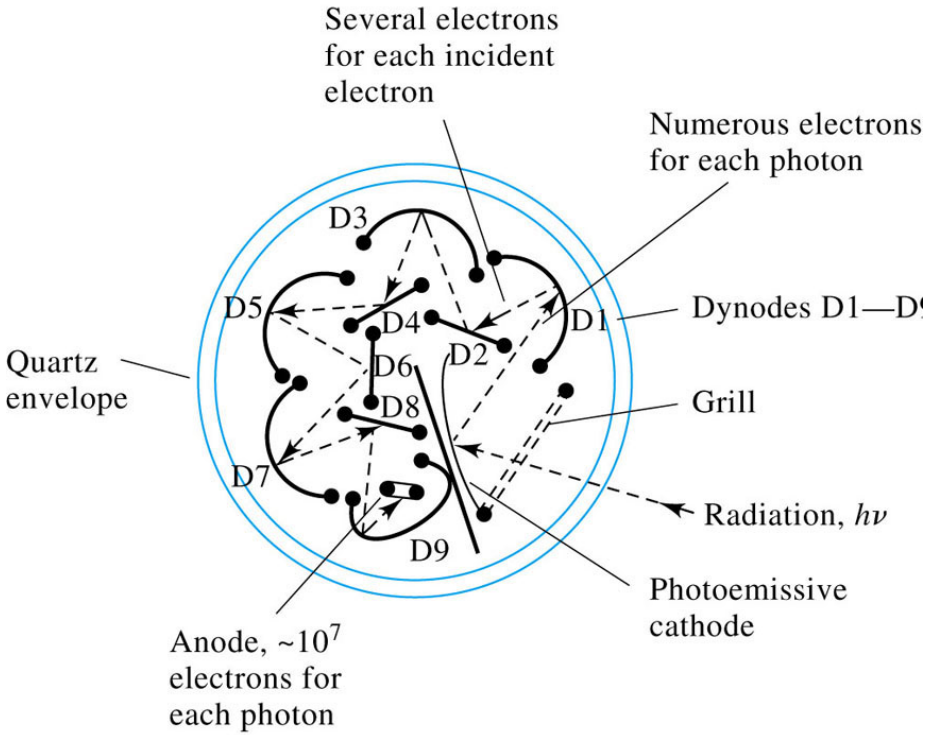

(b)

Photoconductive Detector

Absorption of radiation by semiconductor produces electrons and holes, thus leading to enhances conductivity

The most sensitive transducer for monitoring radiation in the near IR region (0.75 ~ 3 um)

Lead sulfide is the most widely used.

Is important in FT-IR

Multi-channel Photon Detector: PDA

Photodiode Array (PDA)

- The individual photodiodes are a reverse-biased pn junction

- The number of transducer elements in a chip ranges from 64 to 4096 (mostly 1024)

The Advantages of PDA

1. **Various elements of the dispersed spectrum are measured simultaneously**
2. **Fast measurement**

The Shortcomings of PDA

1. **Low sensitivity**
2. **Short dynamic range**

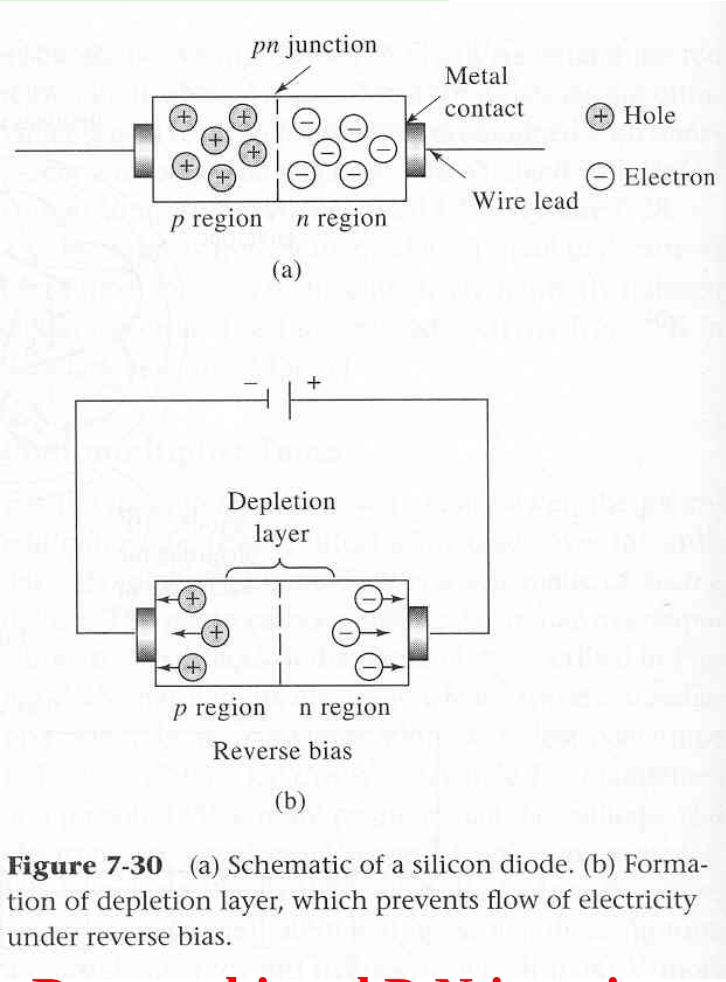

Figure 7-30 (a) Schematic of a silicon diode. (b) Formation of depletion layer, which prevents flow of electricity under reverse bias.

Reverse biased P-N junction

Radiation → holes and electrons in the depletion region

Photodiode Array UV-visible Spectrophotometer

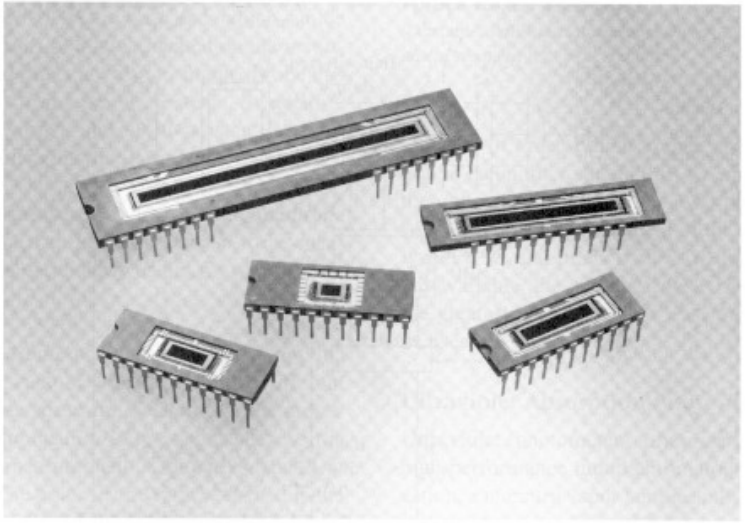

Figure 13-14 Diode arrays of various size. *(Courtesy of EG&G Reticon, Inc.)*

PDA is placed in the focal plane of a spectrometer so that various elements of the dispersed spectrum can be transduced and measured *simultaneously*.

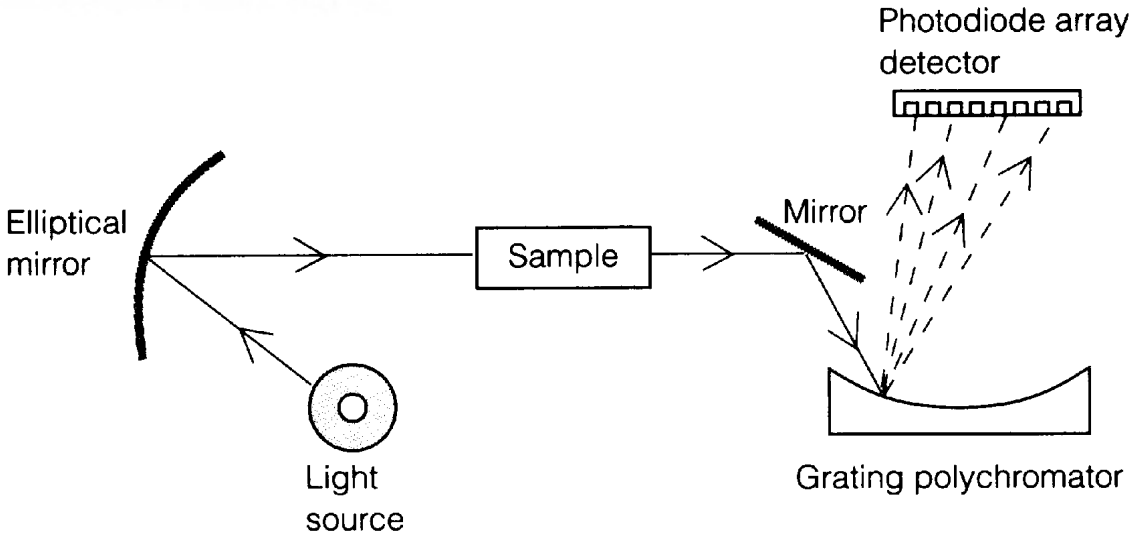

Multichannel Photon Detector: CCD

(2) Charge Coupled Device (CCD)

- 512 X 320 pixels

- Greater sensitivity to lower light level

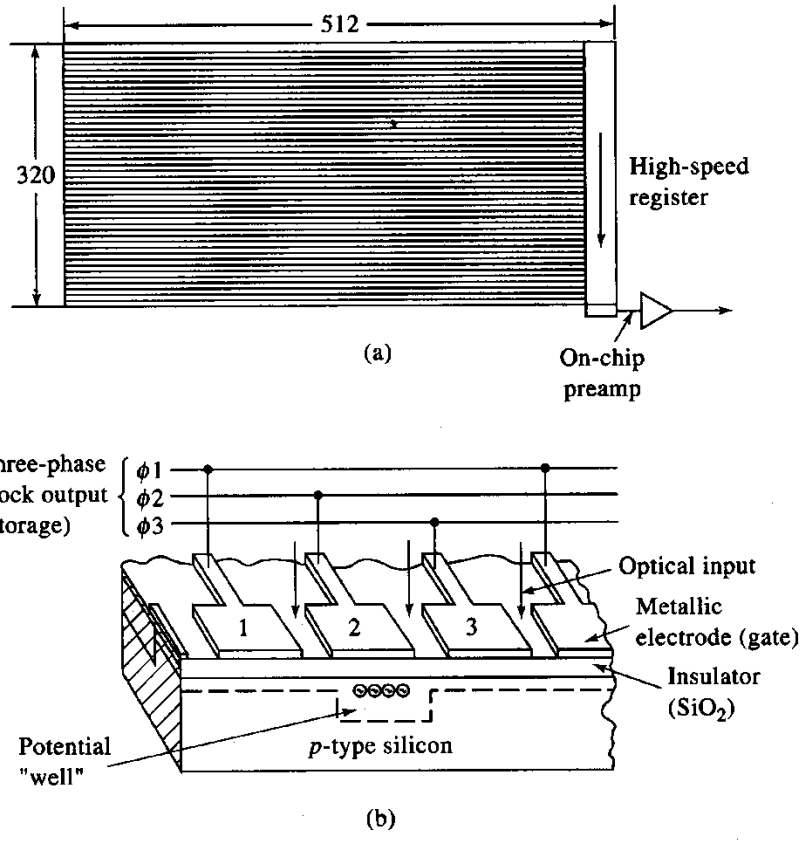

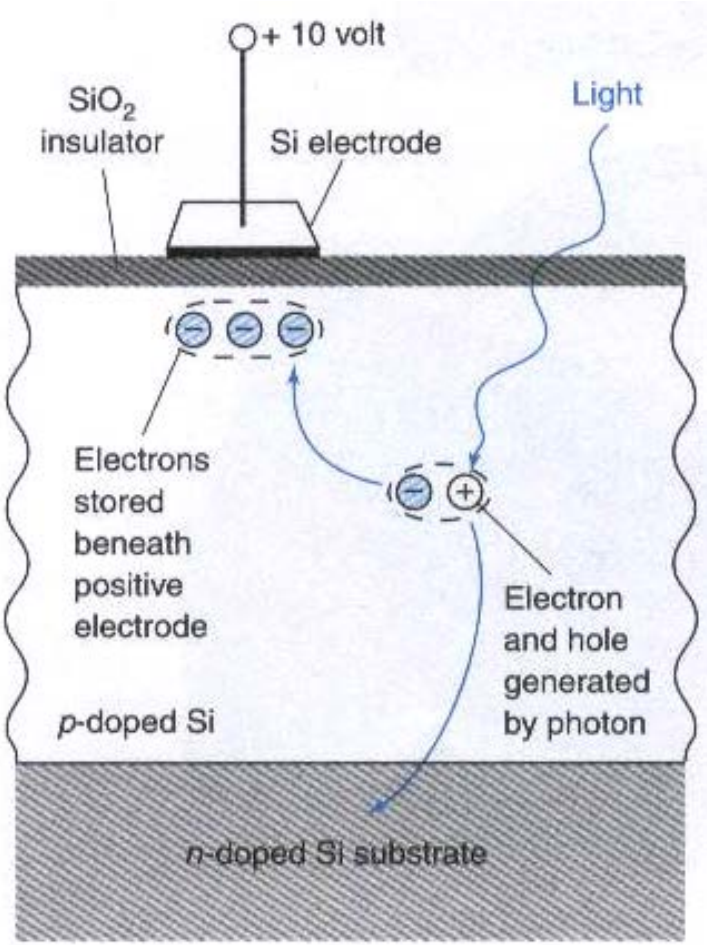

Multi-channel Photon Detector: CCD

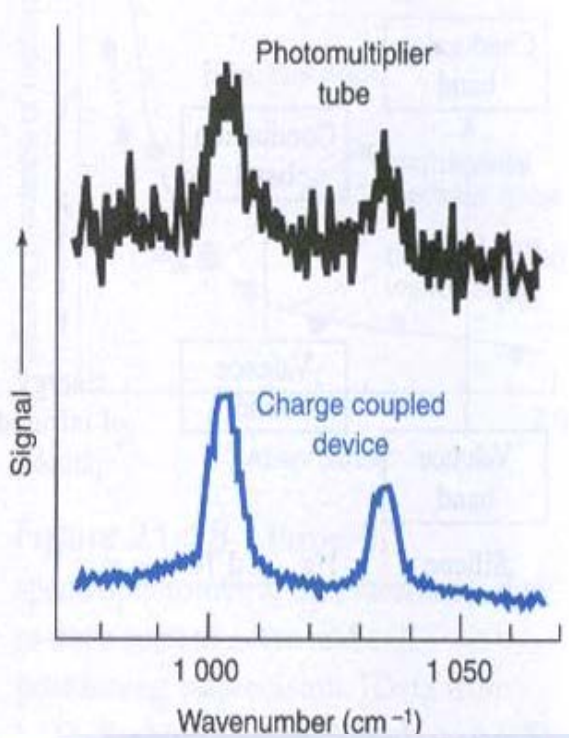

Table 21-2

Minimum detectable signal (photons/s/detector element) of ultraviolet/visible detectors

Signal acquisition time (s)	Photodiode array		Photomultiplier tube		Charge coupled device	
	Ultraviolet	Visible	Ultraviolet	Visible	Ultraviolet	Visible
1	6 000	3 300	30	122	31	17
10	671	363	6.3	26	3.1	1.7
100	112	62	1.8	7.3	0.3	0.2

SOURCE: R. B. Bilhorn, J. V. Sweedler, P. M. Epperson, and M. B. Denton, *Appl. Spectros.* **1987**, *41*, 1114.

Thermal Transducers

- Used in IR (IR photon energy: not enough to produce photoelectron)
- IR: use photoconductivity detector or thermal transducer
- Radiation is absorbed by a small blackbody → temperature raise

I. Thermocouple (or thermopile)

Between the two junctions [copper and constantan (Cu + W)] a potential develops that varies with the difference in temperature of the junctions.

II. Bolometer (or thermistor)

NiO, Pt or semiconductor: high change in resistance as temperature change

III. Pyroelectric Transducer

Photon Counting

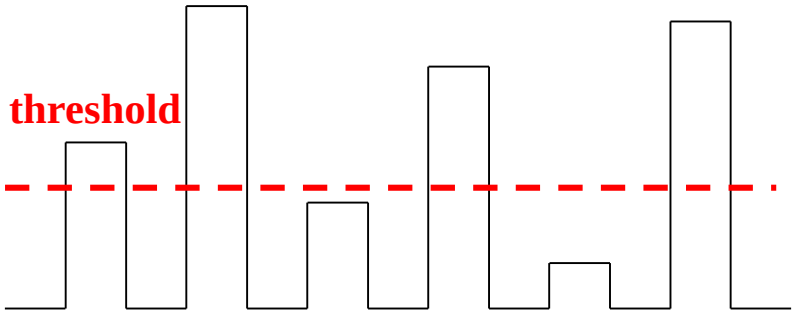

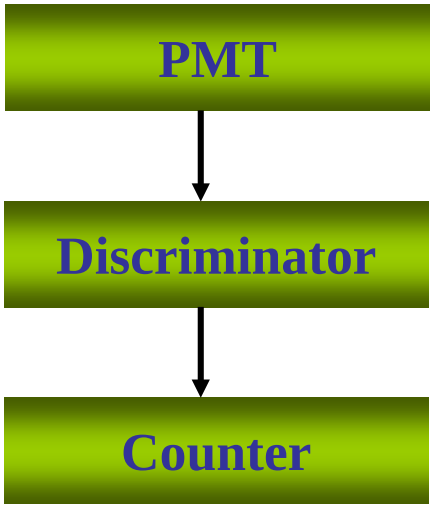

set threshold range

The pulses whose heights exceed an appropriate threshold are counted
: excludes most dark current

Advantages: - improved S/N ratio and sensitivity to lower radiation levels
- less sensitive to PMT voltage and temperature fluctuations
Disadvantages: - equipment is complex and expensive

Application: fluorescence, chemiluminescence, Raman

Anal. Chem. **1995,** *67,* 139−144

Wavelength-Resolved Fluorescence Detection in Capillary Electrophoresis

Aaron T. Timperman, Karim Khatib, and Jonathan V. Sweedler*

Department of Chemistry, University of Illinois, Urbana, Illinois 61801

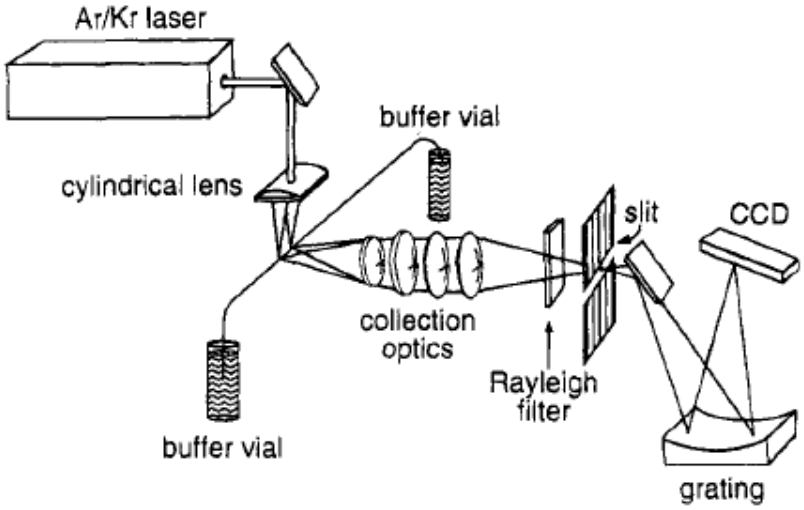

Figure 1. Schematic of the wavelength-resolved laser-induced fluorescence detection system.

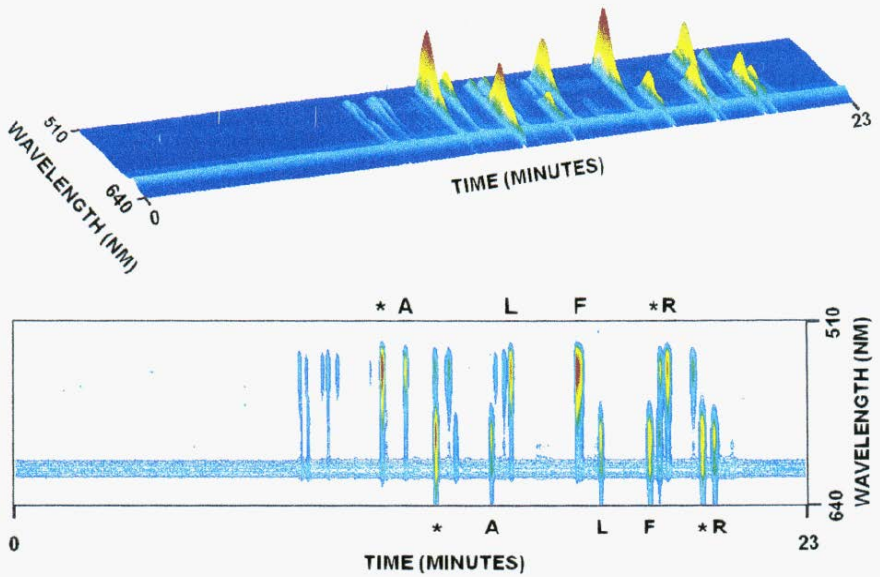

Figure 5. (A, top) Wavelength-resolved electropherogram of a mixture of Bodipy 503/512 C_3 and Bodipy 576/589 C_3 amino acid conjugates. The emission from the Bodipy 503/512 C_3 derivatives appears at shorter wavelengths than the emission from Bodipy 576/589 C_3 derivatives. The continous feature at ~583 nm is the major Raman band of water. (B, bottom) A contour plot of the electropherogram showing the elution order: dye (*), alanine (A), leucine (L), phenylalanine (F), dye (*), arginine (R).

Anal. Chem. **2006,** *78,* 4509−4516

Analysis of the Gas Phase of Cigarette Smoke by Gas Chromatography Coupled with UV-Diode Array Detection

Dimitris G. Hatzinikolaou,[†] Verner Lagesson,[‡] Anastasia J. Stavridou,[†] Aristea E. Pouli,[†] Ludmila Lagesson-Andrasko,[‡] and John C. Stavrides*[,†]

Institute of Biomedical Research and Biotechnology, 55 Solomou Street, 104 32 Athens, Greece, and GC-UV Center, Kobergsgränd 2, SE-587 21 Linköping, Sweden

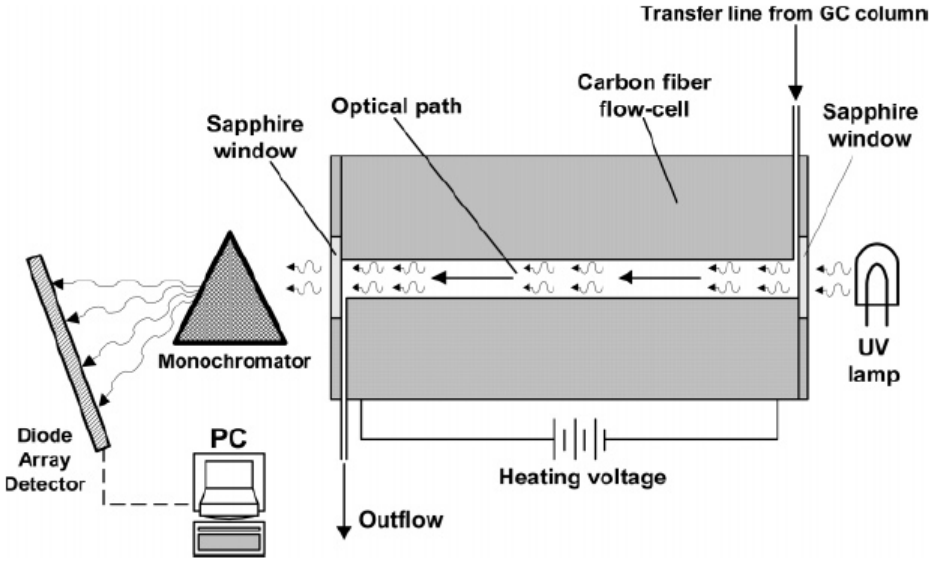

Figure 1. Schematic representation of the UV-diode array detection system.

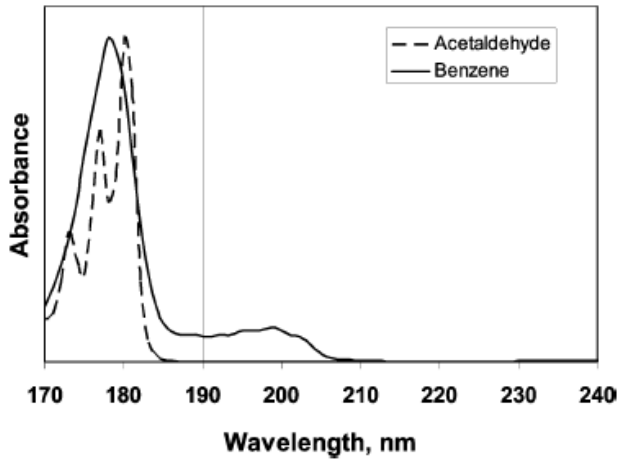

Figure 2. The gas-phase absorption spectra of acetaldehyde and benzene in the short-UV region.

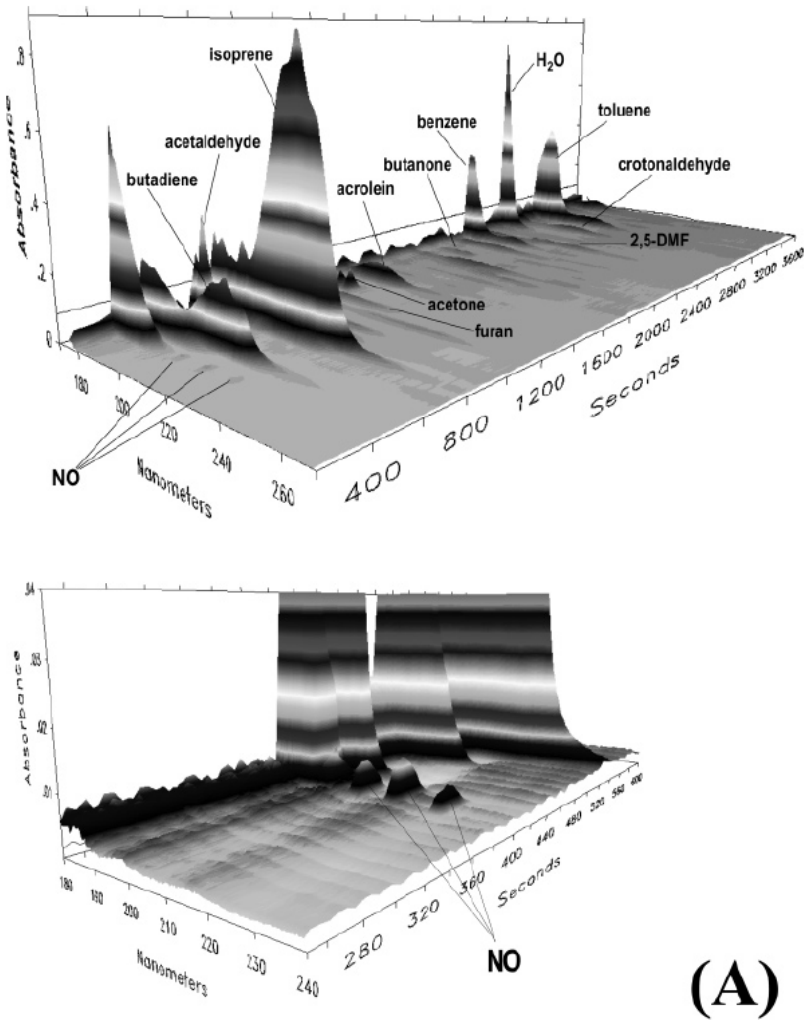

Table 1. Quantification Characteristics for Certain Vapor Phase Compounds

compd	wavelength[a] (nm)	linearity[b] R^2	LOQ[c] (ng)	linear range (up to μg)
nitric oxide	213	0.992	61	140
butadiene	208	0.989	0.76	1.60
acetaldehyde	180	0.952	7.9	27.9
furan	203	0.996	1.6	16.5
isoprene	214	0.978	1.9	4.0
acrolein	194	0.991	3.2	6.8
acetone	193	0.984	3.6	19.3
benzene	178	0.990	0.77	1.84
2-butanone	195	0.988	5.0	22.4
2,5-DMF	206	0.993	4.4	18.6
crotonaldehyde	202	0.996	3.5	20.7
toluene	183	0.995	0.64	1.35

[a] The reported wavelengths correspond to the 2D chromatogram selected for the construction of the calibration curve. [b] Linearity refers to the mean R^2 of the calibration curves prepared for three different flow rates. [c] LOQs were determined on the basis of a signal to noise ratio of 10 and correspond to the current dimensions of the UV detector as well as the minimum flow rate of the system (5 mL/min).

Figure 3. Typical 3D chromatogram of cigarette smoke gas phase, with some characteristic identified compounds. 2 mL from the fourth puff (mixture of eight cigarettes) of Kentucky 1R4F cigarette were directly injected into the system. A. The nitric oxide region of the 3D chromatogram.

Anal. Chem. **2007**, *79*, 8162−8169

Analysis of Neuroactive Amines in Fermented Beverages Using a Portable Microchip Capillary Electrophoresis System

Christine N. Jayarajah, Alison M. Skelley,† Angela D. Fortner, and Richard A. Mathies*

Department of Chemistry, University of California, Berkeley, California 94720

A portable microfabricated capillary electrophoresis (CE) instrument is used for the determination of neurologically active biogenic amines, especially tyramine and histamine, in fermented beverages. The target molecules are labeled on their primary amino groups with fluorescamine in a 10-min reaction, and the samples analyzed directly, producing a detailed electropherogram in only 120 s on a microfabricated glass CE device containing 21.4-cm-long separation channels. Tyramine was found mainly in red wines at <1−3.4 mg/L, while the histamine content of these samples ranged from 1.8 to 19 mg/L. The highest levels of histamine (20−40 mg/L) were found in sake. The analysis of samples drawn from grape crush through malolactic fermentation in four varieties of zinfandel red wines revealed that histamine and tyramine are produced during yeast and malolactic fermentation, respectively. Following malolactic fermentation, the histamine content in these samples ranged from 3.3 to 30 mg/L, and the tyramine content ranged from 1.0 to 3.0 mg/L. This highly sensitive and rapid lab-on-a-chip analysis method establishes the feasibility of monitoring neurologically active amine content and potentially other chemically and allergenically important molecules in our food supply.

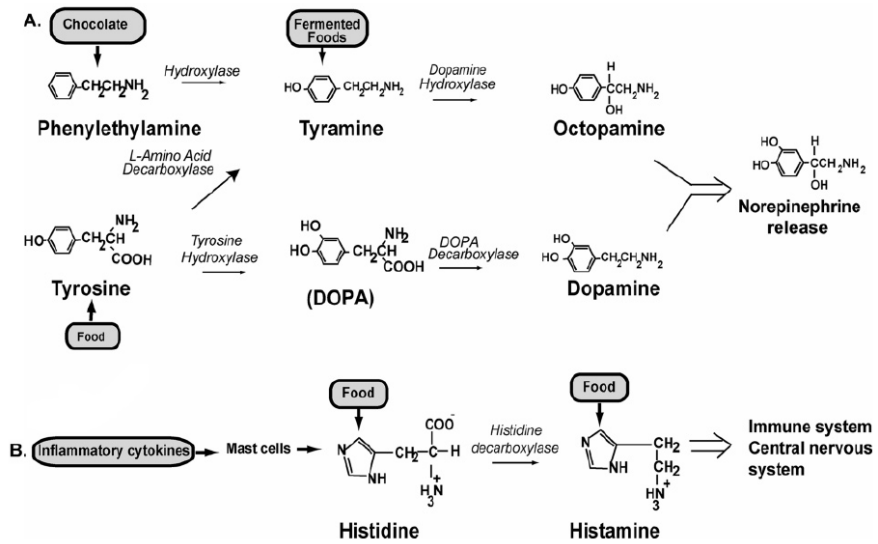

Figure 1. Metabolic pathways that mediate biogenic amine responses. (A) Tyramine is generated from the decarboxylation of tyrosine and from excess plasma levels of phenylalanine and phenyl ethylamine. Monoamine oxidases (MAO) catalyze the oxidative deamination of biogenic amines, reducing the circulating amounts of pressor amines such as tyramine, norepinephrine, epinephrine, and dopamine. Tyramine that is not deaminated can produce octopamine, which displaces norepinephrine from storage vesicles causing hypertension and other sympathomimetic physiological effects. (B) Histamine, the decarboxylation product of histidine, enters the immune and central nervous systems directly from food intake or when released by mast cells in response to allergic reactions, causing edma, itching, hypotension, and bronchoconstriction.

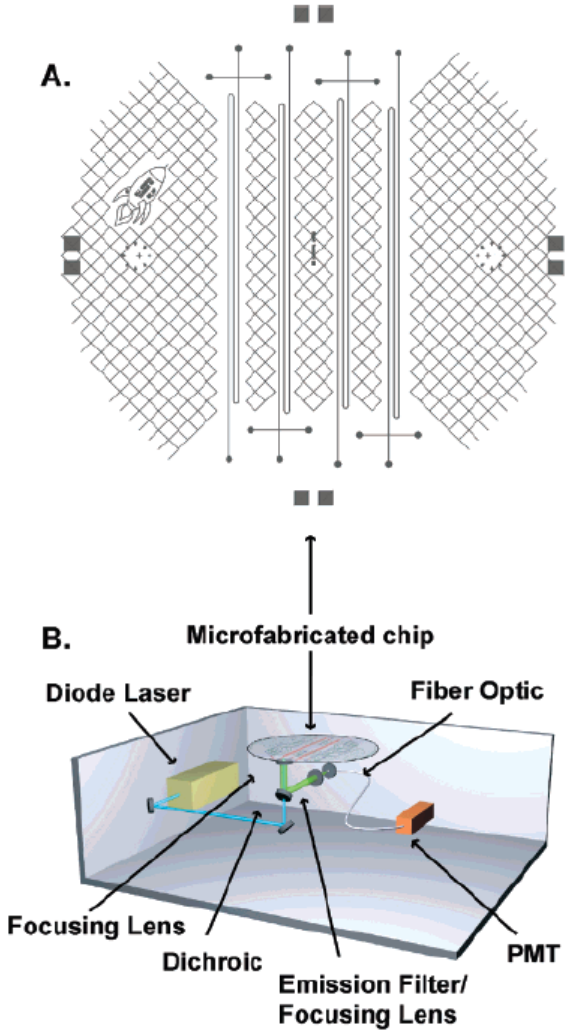

Figure 2. Schematic diagram of the microchip capillary electrophoresis chip and instrument adapted from ref 27. (A) The microfabricated chip consists of four folded separation channels 21.4 cm in length, each with a 0.6-cm-long, 70-μm-wide injection channel placed 0.6 cm from the anode reservoir. The crosshatch marks are included in the chip design for improved bonding. (B) This microchip is placed against the planar face of a composite objective through which the confocal excitation and fluorescence detection is performed. Electrophoresis power supplies, a thermoelectric cooler for temperature control, and pneumatic valve actuators are also contained within the instrument. The 11-kg instrument measures 10 × 12 × 4 in.

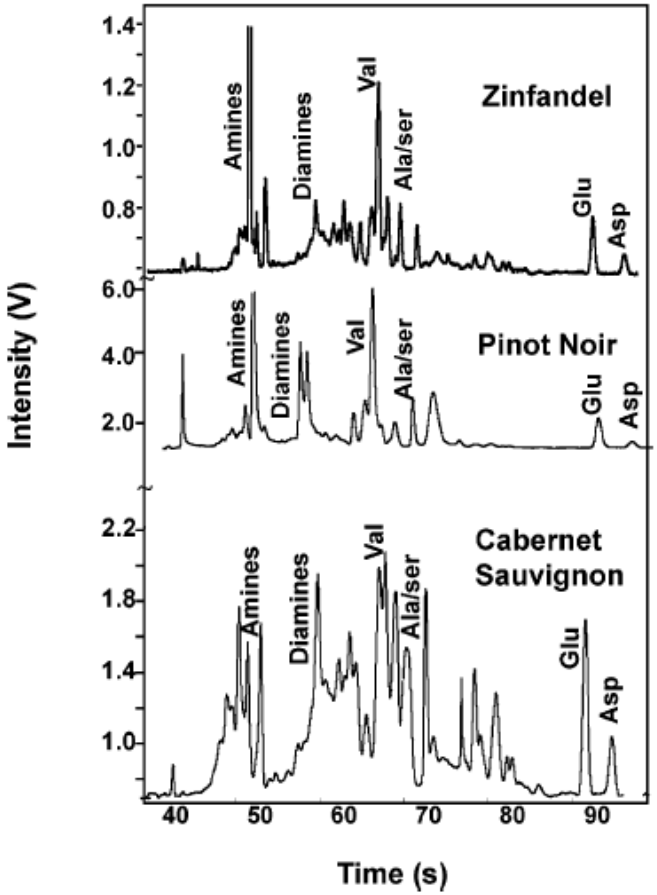

Figure 6. Electropherograms for three different red wine samples (unspiked), all at 50-fold dilution. The traces were aligned in time using the monoamines, valine and glutamic acid peaks.